

DAS Departamento de Automação e Sistemas
CTC Centro Tecnológico
UFSC Universidade Federal de Santa Catarina

Separation of CT-Based CAD-to-Part-comparisons for Dimensional Quality Control

*Monografia submetida à Universidade Federal de Santa Catarina
como requisito para a aprovação da disciplina:
DAS 5511: Projeto de Fim de Curso*

Augusto Schneider Westphal

Florianópolis, agosto de 2013

Separation of CT-Based CAD-to-Part-comparisons for Dimensional Quality Control

Augusto Schneider Westphal

Marcelo Ricardo Stemmer
Orientador do Curso

Acknowledgements

I would like to thank my supervisors, Ricardo Marcelo Stemmer - UFSC - and Christopher Isenberg - WZL - for the support in theoretical concepts and practical work, and also for the attention and guidance in this project.

I also thank the graduate engineer Matheus Gontijo Martins who previously worked on this project as a UFSC student and offered great help in the early stages of adaptation, and the Marter's student Fabricio Borges for helping with CT equipment and its operation.

Finally, I thank my family, my girlfriend Julia and friends for their support during my stay in Germany.

Resumo

A inspeção de peças moldadas por máquinas injetoras engloba métodos convencionais de inspeção como os ópticos e os táteis, os quais possibilitam um feedback importante para a correção da ferramenta de fabricação. No entanto, tais métodos convencionais possuem a chamada correção iterativa, a qual geralmente requer uma grande quantidade de tempo para ser efetuada. Soma-se a esse o fato de algumas peças possuírem partes inacessíveis devido a sua geometria complexa, as quais podem apenas ser acessadas através do corte da peça - o que configura um processo destrutivo.

A Tomografia Computadorizada (TC) aparenta então ser uma potente solução para a inspeção de peças moldadas por injeção, uma vez que se trata de um processo não destrutivo que tem como resultado uma nuvem de pontos de alta densidade. Essa nuvem pode ser utilizada para uma inspeção “peça para CAD”, o que possibilita a medição das partes não acessíveis da peça.

Neste sentido, o projeto tem como objetivo verificar a influência de quatro fatores controláveis de um processo de produção de peças plásticas por meio de máquinas injetoras. Deseja-se definir os parâmetros mais críticos do processo de maneira que o erro dimensional entre as superfícies de interesse das peças produzidas e o modelo CAD seja o mínimo possível. Para tal é proposto um experimento variando os quatro fatores de produção em torno de valores usuais de produção, obtendo assim para cada um deles os níveis baixo, central e alto. A combinação das variações desses quatro fatores resultou na produção das 62 amostras analisadas.

A tomografia computadorizada das amostras permitiu sua reconstrução tridimensional, a qual é utilizada na comparação com seu modelo nominal. Dessa comparação extraíram-se os desvios para cada superfície das amostras, com o auxílio de uma metodologia de separação por ordens (zero, primeira e segunda) e seus parâmetros. Foi gerado então um modelo matemático capaz de representar cada ordem de desvio das superfícies em função dos fatores de entrada.

A partir do modelo foi possível variar os parâmetros de entrada e analisar a intensidade dos desvios nas superfícies, como também a influência individual de cada fator controlável na saída. Por fim, foram levantados os parâmetros de produção que exercem maior influência sobre os desvios em cada superfície. Tal análise poderá

servir para produção comercial com maior precisão dimensional, de acordo com as superfícies de interesse, como também para estudos futuros.

Abstract

The parts inspection by injection molding machines includes conventional inspection methods such as optical and tactile, which enables an important feedback for correction of tool manufacturing. However, these conventional methods have an iterative correction, which usually requires a lot of time to be accomplished. In addition, some pieces have inaccessible parts due to its complex geometry, which can only be accessed by cutting the piece - which configures a destructive process.

Computed tomography (CT) then appears to be a powerful solution for the inspection of injection molded parts, since it is a non-destructive process that results in a point cloud of high density. This cloud can be used for inspection "CAD-to-Part", which allows measurement of non-accessible parts of the piece.

In this sense, the project aims to determine the influence of four controllable factors of a production process of plastic parts by injection molding machines. We intend to define the most critical parameters of the process so that the dimensional error between the surfaces of interest produced parts and CAD model is minimized. To this end it is proposed an experiment by varying the four factors of production to values usual production, thereby obtaining for each of these levels low, middle and high. The combination of the variations of these four factors has resulted in the production of 62 samples.

Computed tomography of the samples allowed a three-dimensional reconstruction, which is used in comparison with its nominal model. From this comparison were extracted deviations for each surface of the samples with the aid of a method of separation by orders (zero, first and second) and its parameters. Was generated then a mathematical model able to represent each order deviation of the surfaces as a function of input factors.

From the model it was possible to vary the input parameters and analyze the surface deviations in intensity, as well as the individual influence of each controllable factor in the output. Finally, were defined the production parameters with most influence on each surface deviation. Such analysis could serve for commercial production with higher dimensional accuracy according to the surfaces of interest as well as for future studies.

Contents

List of Figures	viii
List of Tables	xi
List of Abbreviations	xii
1 Introduction	1
1.1 Project objectives	2
1.2 Methodology	4
1.3 Document Structure	4
2 Plastic Injection Molding Process	6
2.1 Phases of the Injection Molding Process	7
2.1.1 Molding filling	7
2.1.2 Packing	7
2.1.3 Holding	7
2.1.4 Cooling	7
2.1.5 Part ejection	7
2.2 Plastic parts	8
2.2.1 Ultradur B4300 G4	8
3 Fundamentals of X-Ray Computed Tomography	9
3.1 CT measuring operation	10
3.1.1 Settings of CT parameters	10
3.1.2 Setting up the workpiece	11
3.1.3 Measurement	11

3.2	Uncertainty in measurement	12
3.3	CT strengths and limitations	13
4	Design Of Experiments	14
4.1	Benefits of DOE	15
4.1.1	Screening and Optimization	15
4.2	Specification of factors	15
4.2.1	Definition of the standard reference	16
4.3	Specification of responses	16
4.4	Model concept	16
4.4.1	Response Surface Methodology (RSM)	17
4.4.1.1	RSM design	18
4.4.1.2	Samples production	19
4.5	Regression model evaluation	19
5	Response Surface Modeling	21
5.1	CT measurement and alignment	21
5.1.1	Calibration and Qualification	21
5.1.2	Design of a Holder	23
5.1.3	Selection of CT parameters and measurements	25
5.1.4	Calypso	26
5.1.4.1	Best-fit	26
5.1.5	Point clouds	27
5.2	Separation of deviations	28
5.2.1	Mathematical Background	28
5.2.1.1	The 0th order form deviations	29
5.2.1.2	The 1st order form deviations	29

5.2.1.3	The 2nd order form deviations	30
5.2.2	SmartInspeCT	32
5.3	Modeling	35
5.4	CT measurements and RSM comparisons	37
6	Results and Analysis	42
6.1	Surface 1 - Inside	42
6.2	Surface 2 - Bottom	44
6.3	Surface 3 - Triple Cavity	46
6.4	Surface 4 - Upper Strip	48
6.5	Surface 5 - Single Cavity	50
6.6	Surface 6 - Right Side	52
6.7	Analysis of production factors	54
6.7.1	Pressure	55
6.7.2	Pressure time	55
6.7.3	Cooling time	55
6.7.4	Cooling temperature	56
7	Conclusion	57
8	Future Work	58
	References	59
	Appendix A: DOE worksheet	61
	Appendix B: Response surface model relative error (%) compared to measured values	63
	Appendix C: Response surface model and SmartInspeCT comparison	70

List of Figures

1.1	Optimization loop for the tool correction.	2
1.2	Separation methodology.	3
2.1	Schematic representation of a plastic injection tool [13].	6
3.1	Metrotom CT scanner used in this project [9].	9
3.2	Positioning system, X-ray tube and detector [9].	10
3.3	Schematic description of CT operation and reconstruction process. . . .	12
4.1	A symmetrical distribution of experimental points around a center-point experiment.	14
4.2	The worksheet of the application	18
4.3	All 62 produced samples used in this experiment.	19
5.1	Geometric qualification.	22
5.2	Axis qualification.	23
5.3	Holder designed in the software Pro/ENGINEER.	24
5.4	One of the samples being placed in the CT to be measured.	24
5.5	Interface of Metrotom OS while measuring one sample.	25
5.6	CAD model (white) and voxel model (green) before and after best-fit. . .	26
5.7	Color-coded deviation representation of one of analyzed samples. . . .	27
5.8	Point cloud of the sample 1.	27
5.9	Total deviation and separation methodology.	28
5.10	Second order surfaces forms.	31
5.11	SmartInspeCT software with the Bottom surface selected.	33
5.12	SmartInspeCT software results for the Bottom surface selected.	33
5.13	Sample surfaces that have been analyzed in the project.	34

5.14	Deviation of CT samples measurement and response surface model calculated values for Surface 1.	38
5.15	Deviation of CT samples measurement and response surface model calculated values for Surface 2.	39
5.16	Deviation of CT samples measurement and response surface model calculated values for Surface 3.	39
5.17	Deviation of CT samples measurement and response surface model calculated values for Surface 4.	40
5.18	Deviation of CT samples measurement and response surface model calculated values for Surface 5.	40
5.19	Deviation of CT samples measurement and response surface model calculated values for Surface 6.	41
6.1	Offset order deviations for Surface 1 according to factors variation. . . .	43
6.2	First order deviations for Surface 1 according to factors variation. . . .	44
6.3	Second order deviations for Surface 1 according to factors variation. . .	44
6.4	Offset order deviations for Surface 2 according to factors variation. . . .	45
6.5	First order deviations for Surface 2 according to factors variation. . . .	46
6.6	Second order deviations for Surface 2 according to factors variation. . .	46
6.7	Offset order deviations for Surface 3 according to factors variation. . . .	47
6.8	First order deviations for Surface 3 according to factors variation. . . .	48
6.9	Second order deviations for Surface 3 according to factors variation. . .	48
6.10	Offset order deviations for Surface 4 according to factors variation. . . .	49
6.11	First order deviations for Surface 4 according to factors variation. . . .	50
6.12	Second order deviations for Surface 4 according to factors variation. . .	50
6.13	Offset order deviations for Surface 5 according to factors variation. . . .	51
6.14	First order deviations for Surface 5 according to factors variation. . . .	52
6.15	Second order deviations for Surface 5 according to factors variation. . .	52
6.16	Offset order deviations for Surface 6 according to factors variation. . . .	53

6.17	First order deviations for Surface 6 according to factors variation.	54
6.18	Second order deviations for Surface 6 according to factors variation. . .	54
C.1	1st and 2nd orders deviations of CT samples measurement and re- sponse surface model calculated values for Surface 1.	70
C.2	1st and 2nd orders deviations of CT samples measurement and re- sponse surface model calculated values for Surface 2.	70
C.3	1st and 2nd orders deviations of CT samples measurement and re- sponse surface model calculated values for Surface 3.	71
C.4	1st and 2nd orders deviations of CT samples measurement and re- sponse surface model calculated values for Surface 4.	71
C.5	1st and 2nd orders deviations of CT samples measurement and re- sponse surface model calculated values for Surface 5.	72
C.6	1st and 2nd orders deviations of CT samples measurement and re- sponse surface model calculated values for Surface 6.	72

List of Tables

4.1	Minimum, center and maximal factors values to current DOE	16
5.1	Equations for each second order surface form.	31
5.2	SmartInspeCT software output parameters.	34
5.3	Abbreviations of factors	35
5.4	Values of coefficients for each deviation order with response surface full quadratic model of Surfaces 1 to 6.	37
6.1	ANOVA results for Surface 1.	43
6.2	ANOVA results for Surface 2.	45
6.3	ANOVA results for Surface 3.	47
6.4	ANOVA results for Surface 4.	49
6.5	ANOVA results for Surface 5.	51
6.6	ANOVA results for Surface 6.	53
A.1	DOE worksheet with parameters for samples production	62
B.1	Response surface model relative error compared to measured values for Surfaces 1 and 2	65
B.2	Response surface model relative error compared to measured values for Surfaces 3 and 4	67
B.3	Response surface model relative error compared to measured values for Surfaces 5 and 6	69

List of Abbreviations

- DOE - Design Of Experiment
- RSM - Responde Surface Methodology
- WZL - Werkzeugmaschinenlabor
- RWTH - Rheinisch-Westfaelische Technische Hochschule
- CT - Computed Tomography
- CAD - Computer-Aided Design
- ANOVA - Analysis of Variance
- CMM - Coordinate Measuring Machine
- PBT - Polybutylene Terephthalate

1 Introduction

Following specifications and work within satisfactory limits of tolerance are the major challenges of dimensional quality control in production processes. For this reason manufacturing tools such as injection molding require input parameters constantly corrected in order to find an operating point that meets the criteria for the quality of its end products.

The parts inspection provides an important feedback for the tool correction and can thereby reduce the dimensional errors between what is produced and designed. Therefore, the analysis of plastic parts produced by injection molding machines intend to keep the deviations of the surfaces inspected within the tolerance limits: if the deviations are above these stipulated levels is necessary to return the system to its ideal operation point.

Conventional inspection methods such as optical and tactile processes are iterative and usually require a lot of time for their execution, which may result in high production costs. Moreover, in the case of pieces with complex geometry, difficulties in inspecting inaccessible parts are noticed. These parts are only accessed by cutting, resulting in its properties modification - due to internal stresses - and, consequently, introducing a systematic error in the current measurement.

Thus, in order to achieve an optimal dimensional quality in producing parts with increasingly smaller deviations, an optimization loop by using CT can be proposed. The same optimization loop will be used in this project and can be divided into three steps: measurement, comparison and action, as shown in figure 1.1.

With the strategy in place, fours factors of injection molding process were varied around the usual central point and, from the combination of these parameters, 62 samples plastic parts were fabricated and inspected.

Measurement will use CT and 3D reconstruction software. The use of CT is jus-

tified by the characteristic non-destructive process, since the Computed Tomography can access all parts of complex geometry parts. In addition, there is a faster process and less iteration, with provide better accuracy than conventional methods.

In sequence, the **comparison** is performed in software based on numerical computation previously developed for this project. Here we mathematically compare the current measurement with the CAD model of the part, also called nominal model.

Finally, the **action** uses data comparison - deviations - which, along with the input parameters, generate the model that describes a cause-effect relationship. After obtaining the critical factors of production, is provided an analysis which serves to upgrade the machine tool and, therefore, reduce dimensional error of parts.

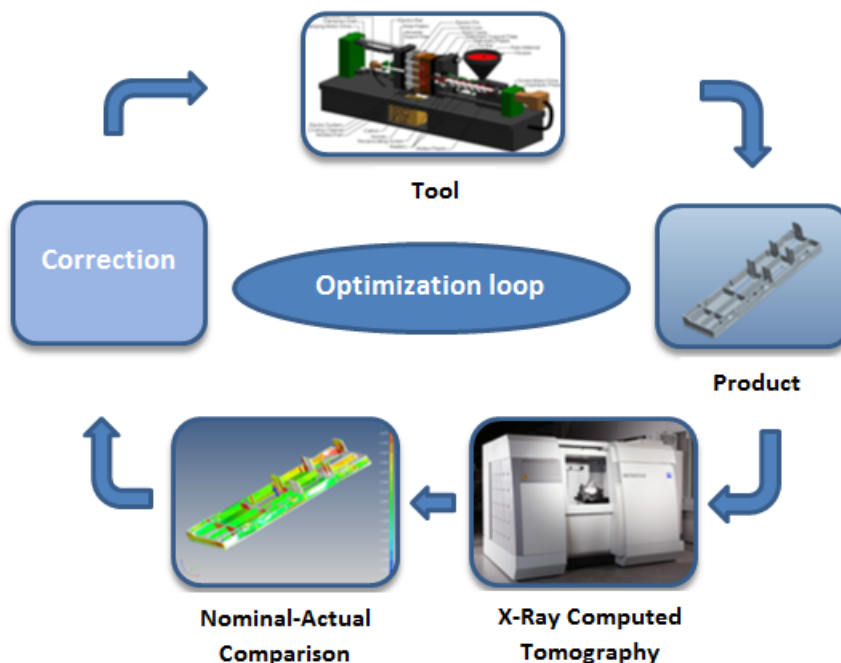


Figure 1.1: Optimization loop for the tool correction.

1.1: Project objectives

The project objective is to determine the influence of four controllable factors of a production process of plastic parts by injection molding machines. We intend to define the most critical parameters of the process so that the dimensional error between the surfaces of interest produced parts and CAD model is minimized. In this sense, the Design of Experiments can be considered in this experiment.

The DOE provides an analysis of the sample surfaces deviations to CAD model when the system is subjected to different values of input parameters and enables to design a model that represents the behavior of the system and simulate the result of changes in factors inputs deviations in output.

In order to quantify the influence of the input parameters in each deviation order a separation approach was used. The separation by orders (zero or offset, first and second) aims to create a database of outputs that will be useful to create the deviations function by using linear regression. The third and higher order deviations will not be considered in this experiment due to the resolution of CT and the uncertainty involved in the process. The figure 1.2 shows the procedure described above:

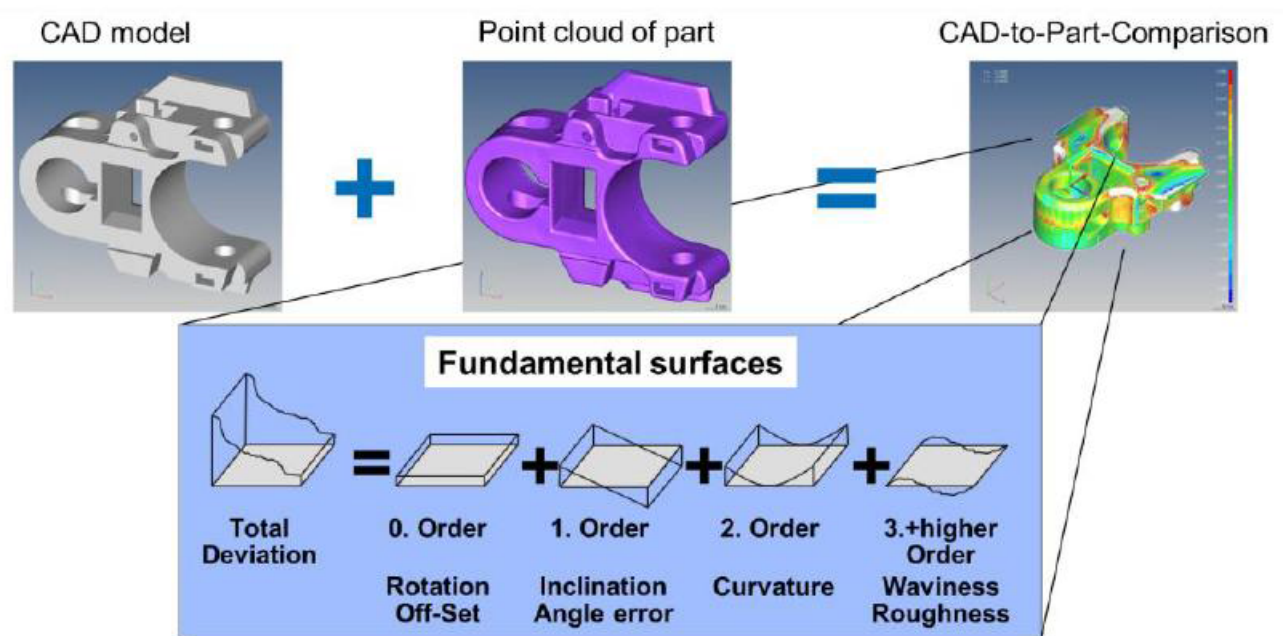


Figure 1.2: Separation methodology.

With the aid of the software SmartInspeCT (previously developed in Matlab) and also the separation methodology, the factors which will be relevant in each deviation order of sample surfaces can be determined. In addition, it is also possible to factors that despite being considered in the experiment are not significant for any order deviation of a specific sample surface and can be considered a noise in the analyses.

1.2: Methodology

The project was developed at the Laboratory for Machine Tools and Production Engineering (Werkzeugmaschinenlabor - WZL) at the RWTH Aachen University. All equipment and technical resources were provided by the institute. The methodology proposed for this project was the following:

- Familiarization with separation approach by orders, CT scanner, software Calypso and CAD-to-Part comparison in software SmartInspeCT;
- Systematic study of DOE, factorial design and response surface model;
- Set-up of a program in Matlab to create and validate the model and also to perform the analysis;
- Measurement, tridimensional reconstruction and alignment to CAD model of 62 samples;
- Analysis and documentation of results.

In a first instance, some references were provided in order to understand the deviations separation approach, the CT fundamentals, software Calypso and the CAD-to-Part comparison in software SmartInspeCT. After the familiarization with the equipment and softwares, some modeling methods were studied and one of them was selected to be used in the evaluating.

After these steps, the program to analyze the deviations and the influence of input parameters was carried out. Therefore, the 62 work pieces were scanned, tridimensional reconstructed and aligned to CAD model using respectively CT and software Calypso. Finally the voxel model was compared with the nominal model using the software SmartInspeCT and then the analyses were performed.

1.3: Document Structure

This document is organized in chapters in the form displayed below:

In chapter 1 an **Introduction** to the project theme and goal is provided. Chapter 2 includes the **Plastic Injection Molding Process** and in chapter 3 the **Fundamentals of X-Ray Computed Tomography** technology are discussed. In chapter 4 are

presented the **Design of Experiment** and solutions chosen for the evaluating; in chapter 5 the **Response Surface Modeling** and the separation approach understanding are given. In chapter 6 **Results and Analysis** are presented from the samples inspection. Finally, in chapters 7 and 8 some **Conclusions** about the current work are presented and possible **Future Work** is discussed.

2 Plastic Injection Molding Process

The plastic injection molding process is an automated process that can be used to produce a wide variety of parts of high quality with great accuracy, very quickly. The process requires basically the use of an injection molding machine, raw plastic material and a mold: the material for the part is fed into a heated barrel, mixed, and forced into a mold cavity where it cools and solidifies to the configuration of the cavity. The steps in this process are described in detail in the next section. A schematic representation of a plastic injection tool follows in figure 2.1.

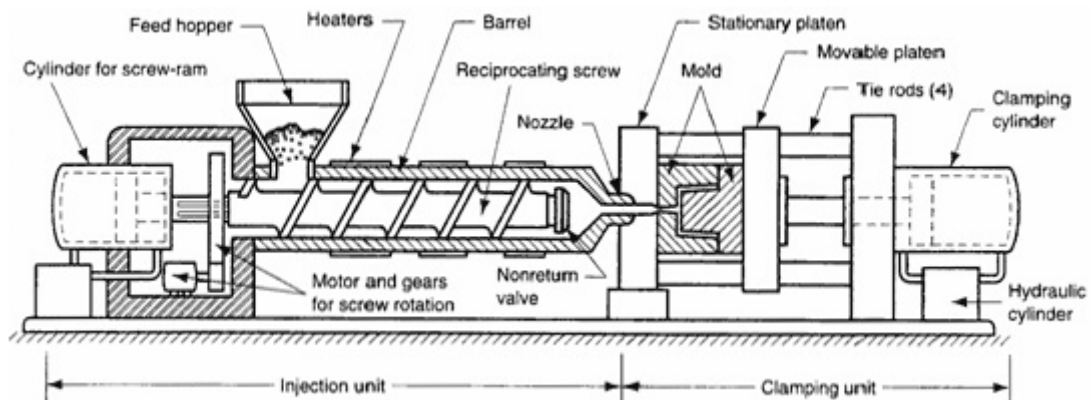


Figure 2.1: Schematic representation of a plastic injection tool [13].

Injection molding is used to produce mainly thin-walled plastic parts for a variety of applications, one of the most common being plastic housings. These housings are used in a variety of products including household appliances, consumer electronics, mechanical parts and automotive dashboards. Other typical applications include different types of open containers such as buckets, toothbrushes, some musical instruments or small plastic toys. Many medical devices, such as valves and syringes, are also manufactured using injection molding.

2.1: Phases of the Injection Molding Process

The plastic injection molding process is the most commonly used manufacturing process for the fabrication of plastic parts and is ideal for producing high volumes of the same object using virtually any plastic material. Though it is a complex process that involves a series of sequential process steps. The different phases of the injection molding process are presented below [1]:

2.1.1: Molding filling

After the mold closes, the melt flows from the injection unit of the molding machine into the relatively cool mold through the feed channel and then into the cavity.

2.1.2: Packing

The melt is pressurized and compressed to ensure complete filling and detailed surface replication

2.1.3: Holding

The melt is held in the mold under pressure to compensate for shrinkage as the part cools. Holding pressure is usually applied until the gate solidifies. Once gate solidification occurs, melt can no longer flow into (or out of) the cavity.

2.1.4: Cooling

The melt continues to cool and shrink with no shrink compensation.

2.1.5: Part ejection

The mold opens and the cooled part is then stripped from the core of cavity, in most cases using a mechanical ejector system.

2.2: Plastic parts

The use of plastics materials offers inherent benefits, as well as some limitations. Within each group of plastics materials different levels of performance are available, and for this reason the correct choice by the product designers is so important and crucial. Some benefits of plastic material are discussed in 1 and presented:

- Versatility;
- Relatively easy to mold into complex shapes;
- Low specific gravity;
- Sometimes transparent;
- Coloring throughout;
- Relatively low energy requirements for processing;
- Chemical resistance;
- Good electrical insulation.

In other hand, high capital investment costs for injection molders and the requirement of highly skilled molding technicians represent some disadvantages of using plastics.

But in general the use of plastics provides cheap, safe and clean plastic parts, e.g. thin walled plastic parts. Thin wall molding reduces resource consumption and cuts weight, reducing fuel usage and carbon emissions in shipping [12]. Some thin wall parts can be made from recyclable plastics such as Polybutylene Terephthalate (PBT). In addition, some Ultraviolet stabilizers and reinforcements such as talc and glass may be mixed.

2.2.1: Ultradur B4300 G4

In this experiment was used the plastic Ultradur B4300 G4 that is an easy flowing injection molding PBT with 20% glass fiber reinforcement for rigid, tough and dimensionally stable parts. It is used to create some things such car door handles, housing for small electric motors, headlight retainers and drum controllers.

3 Fundamentals of X-Ray Computed Tomography

X-Ray Computed Tomography (CT) is a non-destructive technique for visualizing interior features within solid objects, and for obtaining digital information on their 3D geometries and properties. It was initially developed for medical applications and more recently is being used for industrial purposes. In this experiment was used the CT scanner Metrotom 1500, which was developed by the company Carl Zeiss [3.1].

CT scanning utilizes X-ray equipment to obtain cross-sectional images from a work piece in order to produce 3D representations of components. Some of its key uses have been flaw detection, failure analysis, metrology, assembly analysis, and reverse engineering applications.

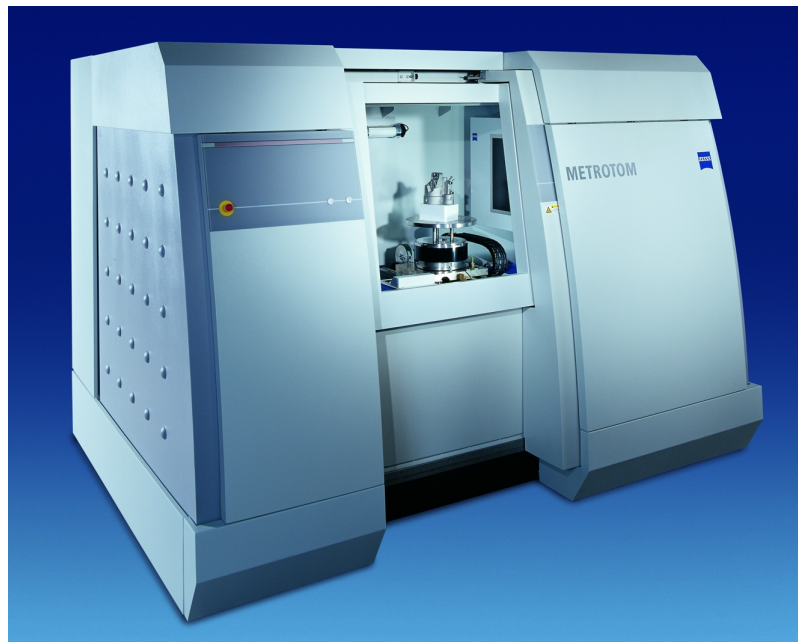


Figure 3.1: Metrotom CT scanner used in this project [9].

Dimensional metrology is the most recent utilization of CT scanners for the industry. It can be used to measure not only the outer but also the inner geometry of work pieces without the need of cutting the work pieces into slices to evaluate hidden or inaccessible features, which is an innovative aspect on metrology [2]. So far CT is the only technology for the holistic quality control of work pieces with non-accessible internal features at very high resolution [3].

In this sense, the main advantages of the CT measurement over the conventional processes such tactile CMM's (Coordinate Measure Machine) or 3D laser scanners are the ability to check non-accessible features for parts with high geometry and the fact of being a non-destructive inspection method.

3.1: CT measuring operation

CT scanner basically consists of a positioning system, a X-ray tube and a detector [3.2]. The correct setup of these components is essential for the proper operation of the CT and good quality of the measurements. Thus the X-ray Computed Tomography has a basic sequence of operation which is presented in the following subsections.

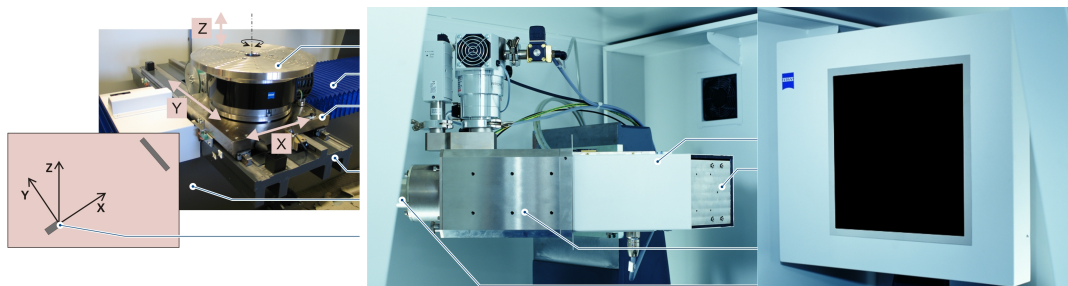


Figure 3.2: Positioning system, X-ray tube and detector [9].

3.1.1: Settings of CT parameters

In a first instance in typical operations, some parameters such as tube voltage, current, integration time, gain and number of projections must be set. The choice of CT parameters affects directly the quality of the reconstruction and needs to be carefully studied.

- Voltage: In an X-ray process, voltage and penetration are directly related. With increasing the X-ray tube voltage, the radiation intensity and the penetration ca-

pability will also increase. It is thus possible to X-ray different materials without problems, e.g. plastics and metals.

Plastics generally do not have high density, so the X-ray emitted by the CT source does not suffer much attenuation, allowing a good reconstruction of the part. In case of denser materials such as metals, it is possible to improve the result of the reconstruction, as well as suppress noise and artifacts by using prefilters.

- **Current:** The X-ray tube current enables the intensification of X-ray radiation by defocusing and optimizes the histogram distribution. The histogram is the frequency distribution of the gray scale values of the detector image.
- **Integration time:** The integration time corresponds to the exposure time of analog cameras. If we increase the integration time, more photons are used for the image measurement. Thus, the image signal is improved without increasing the image blurring. Furthermore, the images become brighter. The measuring time increases also with increasing integration time.
- **Gain:** The gain has an effect on the image signal and the image blurring. If we increase the gain, the image signal and the image blurring increase proportionally. Thus, the image becomes brighter and noisy. This measure does not influence the measuring time.
- **Number of projections:** The number of projections influences the time and quality of part reconstruction.

3.1.2: Setting up the workpiece

The workpiece must be set up on the rotary table in such a way that all projected images of the workpiece are located inside the reconstruction area when a 360° rotation is performed. In this sense, a holder was developed and will be presented in the chapter 5.

3.1.3: Measurement

A X-ray source inside the CT machine emits X-rays that penetrate the part and are attenuated according to the part geometry, density, material and X-ray energy. A

detector placed behind the rotary table is used to record the intensity of the attenuated x-rays. The detector provides a bi-dimensional grayscale image representing the amount of attenuation of the current projection.

After several attenuation images from different rotation angles are obtained it is possible to create, through a mathematical reconstruction, a 3D voxel model (equivalent 3D of the pixel) in which the voxel gray value represents the absorvity of the material. This 3D voxel model can be used to generate a 3D data set (point cloud) of the current scanned part. A schematic figure of the CT measurement described above is shown in figure 3.3.

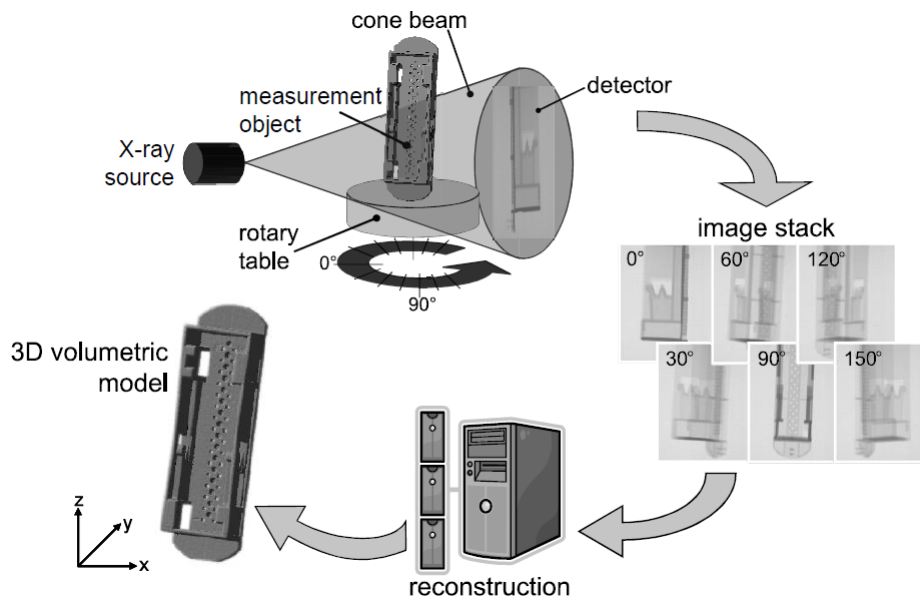


Figure 3.3: Schematic description of CT operation and reconstruction process.

3.2: Uncertainty in measurement

The uncertainty of a CT measurement varies with the input parameter values used for each measurement. It is very difficult to calculate analytically the uncertainty in measurement of CT systems due to the existence of various factors and their interactions that would have to be considered.

However, experimental investigations considering probing deviations have been performed for custom-designed standards, e.g. step cylinders, ball bars or titanium calotte cubes and a cylinder head [4]. According to an experiment with calibrated work pieces proposed by [4], the variation of the parameters made the standard deviation derived from five repetitions varies between approximately 1 and 7.5 μm .

The mentioned experiment has shown how the CT measurement uncertainty range can vary with the set of the parameters for each sample to be measured, and give us an idea about the uncertainty of the computed tomography system.

3.3: CT strengths and limitations

Computed Tomography provides an entirely non-destructive 3D imaging and a conservative reconstruction, allowing sub-voxel level details to be extracted. CT also requires little or no sample preparation, which can lead to cost reduction.

On the other hand, CT has a limited resolution to about 1000-2000x the object cross-section diameter - high resolution requires small objects. This finite resolution causes some blurring of material boundaries. The difficulties of calibration of gray levels to attenuation coefficients complicated by polychromatic X-rays are also a negative aspect. Not all features have sufficiently large attenuation contrasts for useful imaging.

CT scanning is also characterized by the presence of artifacts that can complicate data acquisition and interpretation. Large objects cannot be penetrated by low-energy X-rays, reducing resolving capability. Finally, large data volumes can require considerable computer resources for visualization and analysis. In this sense, the experiments demand computers with high processing and storage capacities 10.

4 Design Of Experiments

This experiment aims to “understand” the process as a whole in the sense that is intended, after design and analyze, to have in hand a ranked list of important through unimportant factors that affect the deviation surfaces.

In this regard, the Design of Experiments (DOE) appears to be a powerful solution, which provides a systematic and rigorous approach to engineering problem-solving that applies principles and techniques at the data collection stage so as to ensure the generation of valid, defensible, and supportable engineering conclusions. In addition, all of this is carried out under the constraint of a minimal expenditure of engineering runs, time, and money.

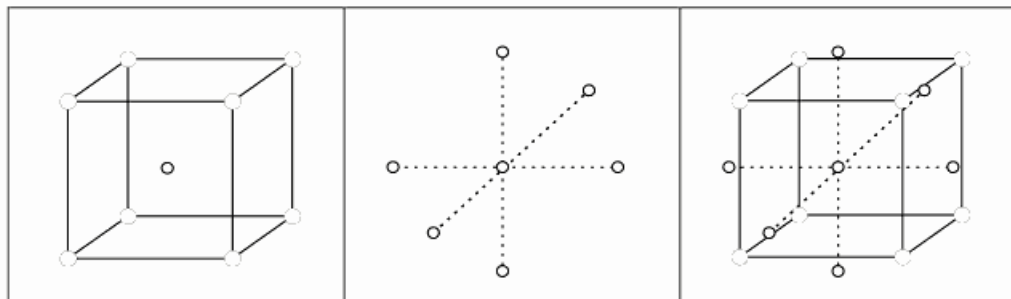


Figure 4.1: A symmetrical distribution of experimental points around a center-point experiment.

DOE involves making a set of experiments representative with regards to a given question. The way to do this is problem dependent, and the shape and complexity of a statistical experimental design may vary considerably. A common approach in DOE is to define an interesting standard reference experiment and then perform new, representative experiments around it (figure 4.1). These new experiments are laid out in a symmetrical fashion around the standard reference experiment in order to evaluate and model the behavior of the system in its vicinity. Hence, the standard reference experiment is usually called the center point [6].

With the aid of this approach, it is possible to create functionally the process modeling with the output being a estimated fitting mathematical function, composed of coefficients with maximal accuracy.

4.1: Benefits of DOE

The great advantage of using DOE is that it provides an organized approach, with which it is possible to address both simple and tricky experimental problems. The experimenter is encouraged to select an appropriate experimental objective, and is then guided to devise and perform a set of experiments, which is adequate for the selected objective.

Thus, by means of DOE, one obtains more useful and more precise information about the studied system, because the joint influence of all factors is assessed.

4.1.1: Screening and Optimization

Screening and Optimization are the first stages of DOE methodology and will be used on this project. They are useful to explore factors in order to reveal whether they have an influence on the responses, and to extract detailed information about them.

4.2: Specification of factors

In DOE the first experiment procedure is to specify the input factors. The important parameters of this experiment have already been identified previously. All four factors used to evaluate the project are controllable and quantitative and expressed in the international system of units and their derivatives. The four injection molding factors are presented below:

- Pressure [bar]
- Pressure time [s]
- Cooling time [s]
- Cooling temperature [°C]

4.2.1: Definition of the standard reference

Ideally each factor should be explored at five levels to allow a reliable quadratic model. But, there are also good optimization designs available, which utilize only three level per explored factor. In this sense, the standard reference has three level and is a known operation point by WZL and was used in this experiment.

The values of the minimum, center and maximum for each input factor can be found in table 4.1. The first factor, pressure used in plastic injection, is varied between 100 and 350 bar. The second factor, pressure time, is varied between 2 and 7 s. The cooling used to cool the mold is represented by two factors. Cooling time is varied between 10 and 20 s and cooling temperature is varied between 30 and 70 °C.

Factors	Min	Center	max
Pressure [bar]	100	225	350
Pressure time [s]	2	4.5	7
Cooling time [s]	10	15	20
Cooling temperature [°C]	30	50	70

Table 4.1: Minimum, center and maximal factors values to current DOE

4.3: Specification of responses

It is important to select responses that are relevant to the experimental goals. In the sample surfaces, the root mean square (RMS) values of deviation orders (zero or offset, first and second) are the most important properties and were selected to be analyzed. As mentioned in chapter 1, the third and higher order deviations will not be considered in this experiment due to the resolution of CT and the uncertainty involved in the process.

The deviation orders were extracted by using the software SmartInspeCT, which was previously developed in WZL for using in this project. The mathematical background of separation will be presented in the next chapter.

4.4: Model concept

Modeling systems can reveal the nature of the relationship between few factors and the measured responses. For some factors and responses the relationship might

be linear, for others non-linear, that is, curved. For some factors and responses exists a positive correlation, for others a negative correlation. These relationships are conveniently investigated by fitting a quadratic regression model.

Models are not reality and will never represent a system perfectly, but approximate representations of some important aspects of reality. It constitutes an excellent tool for understanding important mechanisms of the reality, and for manipulating parts of the reality according to a desired outcome [6].

According to 8, when input factors can be varied across a continuous range of values, the response surface methods may be used. This approach provides designs and models for working with continuous factors and can describe the responses as functions. Thus, the current project uses this methodology.

4.4.1: Response Surface Methodology (RSM)

Response surface methodology consist of a group of mathematical and statistical techniques used in development of an adequate functional relationship between a response of interest and a number of associated control variables. In general, such a relationship is unknown but can be approximated by a low-degree polynomial model of the form:

$$y = f'(x)\beta \quad (4.1)$$

The purpose of considering a low-degree model is to predict response values for given settings of the control variables and to determine, through hypothesis testing, significance of the factors whose leves are presented by the input parameters.

For the current analysis, a second-degree polynomial form was performed by using the full-quadratic response surface regression model, as the following equation:

$$\delta = \beta_o + \sum_i \beta_i x_i + \sum_{i < j} \sum_j \beta_{ij} x_i x_j + \sum_i \beta_{ii} x_i^2 \quad (4.2)$$

Where *delta* represents the RMS deviation (output) and *x* values are the input parameters. The values of *beta* are the coefficients of the function and were extracted from a quadratic regression performed in Matlab. These coefficients will be presented in the next chapter.

4.4.1.1: RSM design

After the standard reference and modeling have been defined, the factors were varied around it with the statistical software Minitab 14 in order to generate a worksheet with the input factors of the samples.

The response surface is a regression model that requires many experiments per varied factor. Good RSM designs should give rise to a model with small prediction error, that means that the design must also contain replicated experiments enabling the performance of a lack of fit test. Therefore, in order to generate a worksheet with the input factors of the samples, a new response surface design was created.

The input factors were varied around the standard reference with the statistical software Minitab 14, with a central composite, in a half gesign, and gave the output of 62 samples.

The worksheet (figure 4.2) is a display of the input factors values, and each one of the 62 samples has different combinations of these parameters values. The complete worksheet is shown in Appendix A.

	C1	C2	C3	C4	C5	C6	C7	C8
	StdOrder	RunOrder	PtType	Blocks	Innendruck	Nachdruckzeit	Kühlzeit	Kühlmitteltemperatur
1	52	1	-1	1	225,0	4,50	10,0	50
2	5	2	1	1	162,5	3,25	17,5	40
3	1	3	1	1	162,5	3,25	12,5	40
4	38	4	1	1	162,5	5,75	17,5	40
5	50	5	-1	1	225,0	2,00	15,0	50
6	30	6	0	1	225,0	4,50	15,0	50
7	45	7	1	1	287,5	3,25	17,5	60
8	35	8	1	1	287,5	5,75	12,5	40
9	9	9	1	1	162,5	3,25	12,5	60
10	11	10	1	1	162,5	5,75	12,5	60
11	32	11	1	1	162,5	3,25	12,5	40
12	41	12	1	1	287,5	3,25	12,5	60
13	12	13	1	1	287,5	5,75	12,5	60
14	49	14	-1	1	350,0	4,50	15,0	50
15	18	15	-1	1	350,0	4,50	15,0	50
16	61	16	0	1	225,0	4,50	15,0	50
17	36	17	1	1	162,5	3,25	17,5	40
18	48	18	-1	1	100,0	4,50	15,0	50
19	31	19	0	1	225,0	4,50	15,0	50
20	21	20	-1	1	225,0	4,50	10,0	50
21	56	21	0	1	225,0	4,50	15,0	50
22	8	22	1	1	287,5	5,75	17,5	40
23	62	23	0	1	225,0	4,50	15,0	50
24	2	24	1	1	287,5	3,25	12,5	40
25	15	25	1	1	162,5	5,75	17,5	60
26	25	26	0	1	225,0	4,50	15,0	50
27	4	27	1	1	287,5	5,75	12,5	40

Figure 4.2: The worksheet of the application

4.4.1.2: Samples production

The samples were manufactured by BOIDA Kunststofftechnik GmbH following the worksheet of input factors presented above. The factors Pressure, Pressure time, Cooling time and Cooling temperature could be directly set and were not an issue. All samples were produced with three replications, but only one of these was in fact analyzed in WZL. The 62 samples used are displayed in the figure 4.3.



Figure 4.3: All 62 produced samples used in this experiment.

4.5: Regression model evaluation

For a regression model analysis and evaluation, it is necessary a basis of statistical testing, which can be performed by using an analysis of variance (ANOVA). ANOVA makes it possible to formally evaluate the performance of models.

ANOVA is a particular form of statistical hypothesis testing - method of making decisions using data - heavily used in the analysis of experimental data. With the aid of ANOVA, is it possible to confirm which factors are significant in each degree of deviation.

This evaluation will be performed in software Matlab by using the generated coefficients and models. With the models, it is possible to simulate inputs and outputs

in order to analyze the behavior of deviations varying the input factors in an appropriate range. The ANOVA analysis will be presented in the chapter 6.

5 Response Surface Modeling

A Response surface modeling was performed in order to investigate the influence of the input parameters in the deviations of each surface of interest. For this purpose, the 62 samples produced were measured in the CT scanner and then aligned to the CAD model.

After aligning the pieces, a high density point clouds were generated and have been used in the separation of the deviations. With deviations acquired, it was possible to generate the coefficients of the model using a quadratic regression and then compare the response surface model performance with the original system. The steps above will be presented one by one in this chapter and at the end some comparison charts are displayed.

5.1: CT measurement and alignment

The first task when measuring a sample with CT is to calibrate and qualify the positioning system. After, we have to find a way to hold the part in the CT rotational desk. The next step is to define the CT parameters and then it is possible to start the measurements.

With the aid of software Calypso - developed by Carl Zeiss, an alignment between the CAD model of the part and voxel model can be done by using the best-fit function. Finally, a second high-density point cloud is generated and used in the comparison performed by the software SmartInspeCT.

5.1.1: Calibration and Qualification

The detector calibration analyzes the response behavior of the detector for different tube voltages and currents and homogenizes the active detector field. A check is

made as to see whether there are any bad pixels [9]. For this purpose, a measuring run is integrated in the software Metrotom OS and was performed monthly in this project.

All of the relevant geometric properties of the CT are determined with the help of a geometric qualification test piece. This is an important prerequisite for optimal reconstruction of the object and was also performed (figure 5.1).

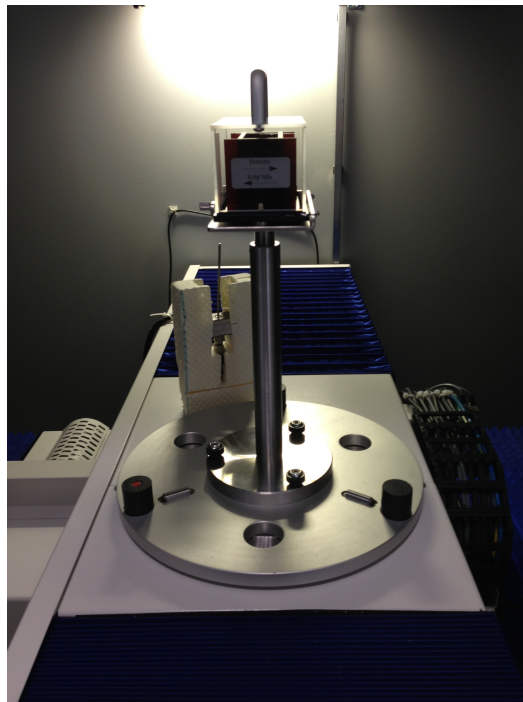


Figure 5.1: Geometric qualification.

An axis qualification (figure 5.2) should always be performed after a geometric qualification especially to prevent a “double margin” in a artifact-free reconstruction. It was performed with the aid of a phantom, as presented in the figure 5.2.

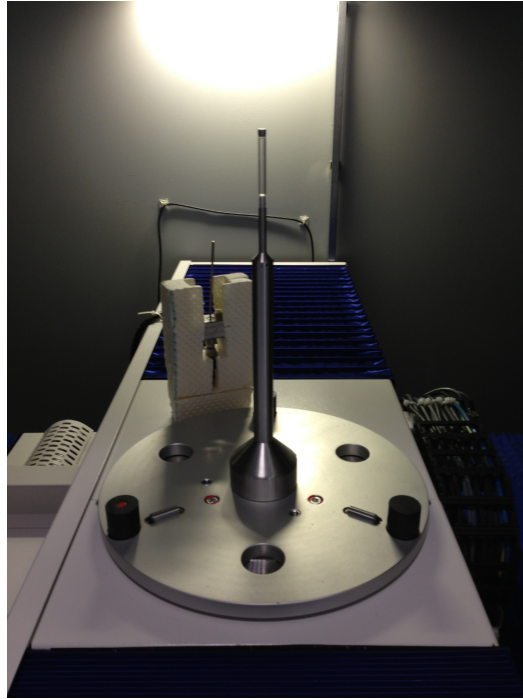


Figure 5.2: Axis qualification.

5.1.2: Design of a Holder

A important task when measuring a sample with the CT is to find a way to hold the part in the CT rotational desk. In this case, the sample cannot have perpendicular edges with the CT X-ray emission source, and any object used to hold the sample could overlap the sample and prejudice the measure result.

To solve this problem, a holder made of low density sponge was proposed in the software Pro/ENGINEER to hold the sample (figure 5.3). How the density of the sponge is much less than the plastic, it did not detracted the reconstruction quality.

For optimal detection and reconstruction, as well as a good penetration of X-rays, the angle measurement should be between 70° and 80° . In this sense the angle of the holder was fixed in a value of 76.50° .

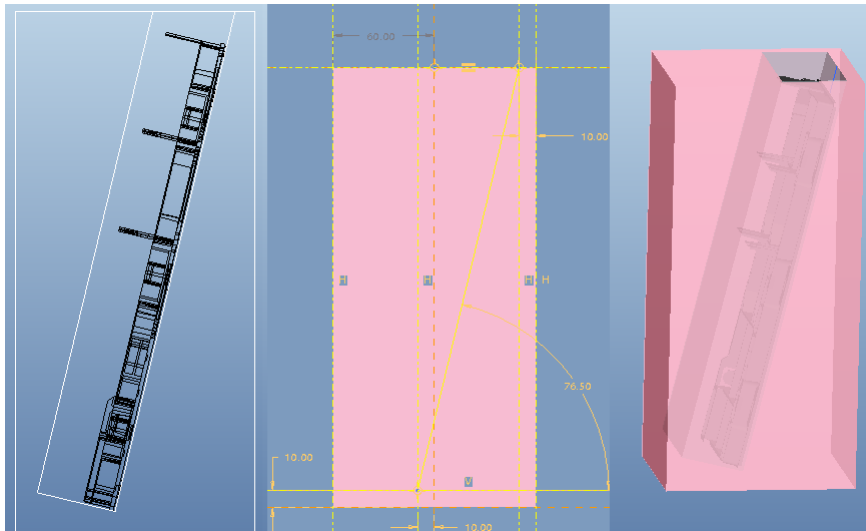


Figure 5.3: Holder designed in the software Pro/ENGINEER.

However, it was not possible to manufacture this holder due to unavailability of the machine tool required. Thus another holder was developed manually with a measurement angle of 70° , which is also considered for optimal measurement.

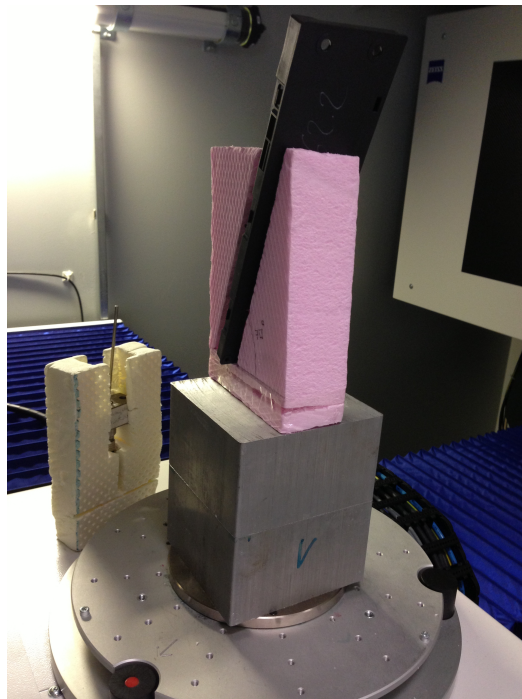


Figure 5.4: One of the samples being placed in the CT to be measured.

5.1.3: Selection of CT parameters and measurements

The next task is to define the CT parameters, such a voltage, the current, an integration time, sensor gain, number of projections, pre-filter, etc. It was defined with the assistance of 11, as follows:

- Voltage: 110 kV;
- Current: 550 μ A;
- Integration time 1000 ms;
- Gain: 16x;
- Number of images: 500;
- Pre-filter: 0 (no pre-filter).

After the CT parameters have been defined, the measurements can now be performed in the software Metrotom OS. An interface of this software is displayed in the figure 5.5. The 62 samples were measured with the aid of the holder that was described before.

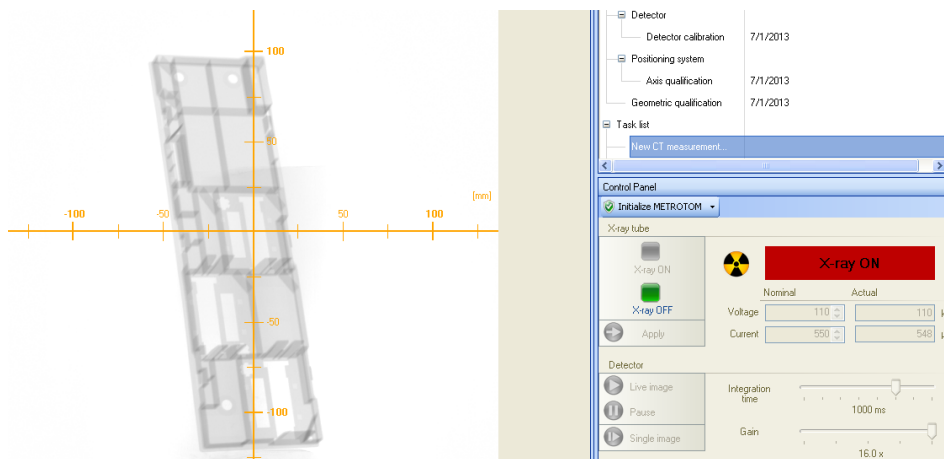


Figure 5.5: Interface of Metrotom OS while measuring one sample.

The CT provides a point cloud with very high point density, which can be used to calculate a 3D surface model. This CT reconstruction has been analyzed at the software VG Studio Max and was considered adequate to the measurement of all of the samples with those parameters.

5.1.4: Calypso

After the reconstruction, the 3D surface model and the CAD model can be used to create a new actual model in the software Calypso. This actual model is a result of the alignment between those two data sets, by using the best-fit function.

5.1.4.1: Best-fit

Best-fit is an algorithm that starts with two data sets and an initial estimate of the aligning rigid-body transform. It then iteratively refines the transform by alternately choosing corresponding points in the meshes and finding the best translation and rotation that minimizes an error metric based on the distance between them [7].

The best-fit function was performed in the standard method, by using the manual run. The figure 5.6 shows the CAD and voxel models before and after best-fit. As mentioned above, the result of the best-fit function is the actual model, which is described as a new point cloud.

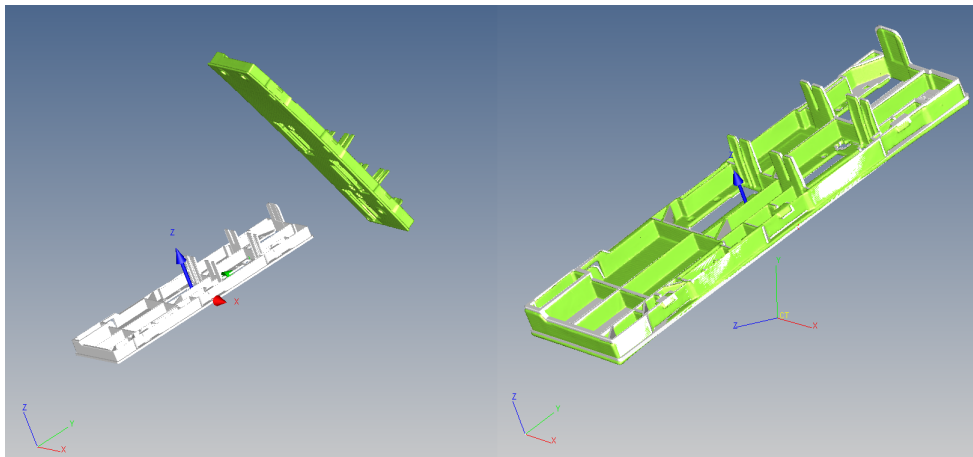


Figure 5.6: CAD model (white) and voxel model (green) before and after best-fit.

The best-fit function in Calypso can also provide a color-coded deviation representation. This function serves merely as illustration and is shown in the figure 5.7 below:

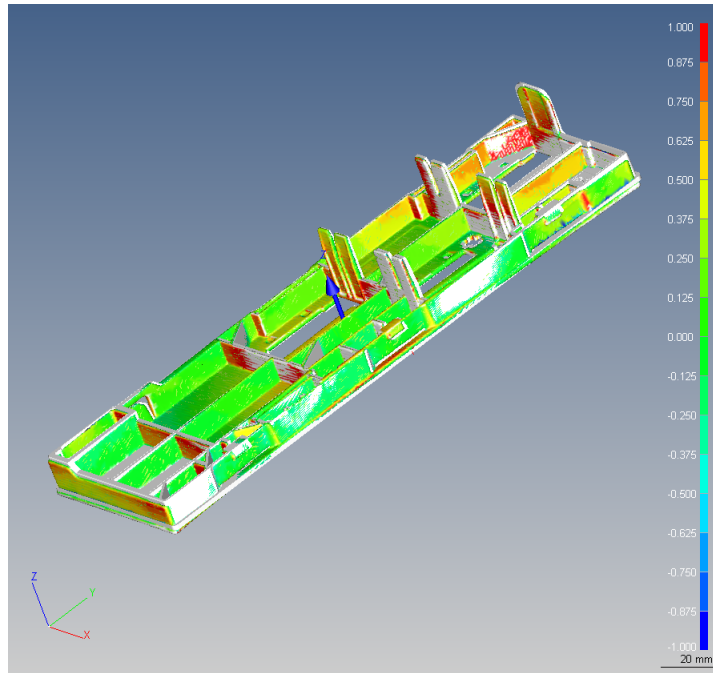


Figure 5.7: Color-coded deviation representation of one of analyzed samples.

5.1.5: Point clouds

A new high density point cloud - .txt file - was created for each sample measured (figure 5.8). The point cloud contains the actual points in the xyz coordinates obtained from the alignment of the real part. This point cloud will be useful to separate the deviations by order in a nominal-actual comparison.

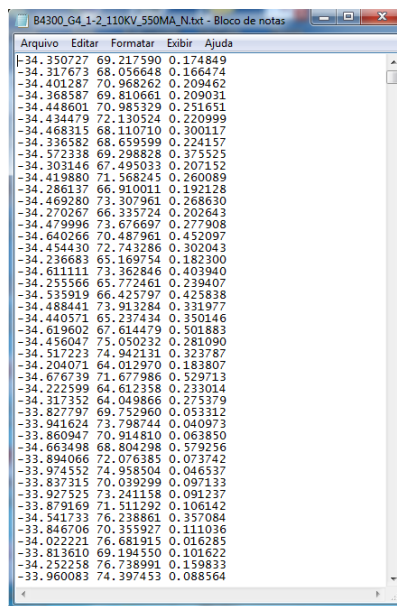


Figure 5.8: Point cloud of the sample 1.

5.2: Separation of deviations

The deviations between a nominal and actual surface can be considered as an overlaid of several order of geometric deviations (offset, slope, curvature, waviness) (figure 5.9). These geometric deviations will be separated to figure out their causes (tool geometry and injection molding process) more easily [3].

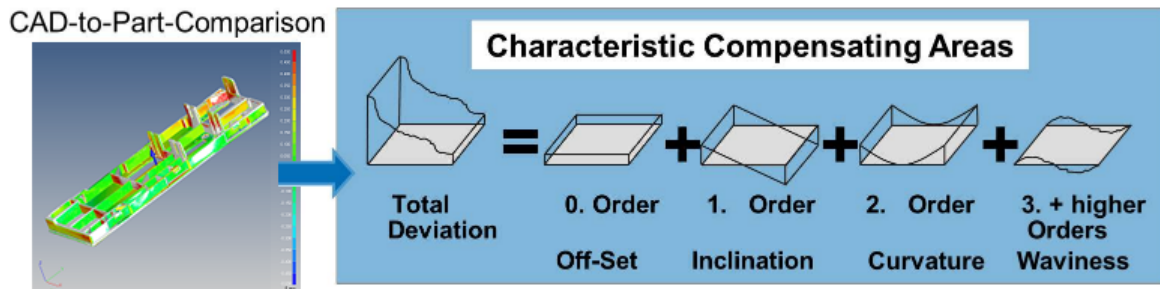


Figure 5.9: Total deviation and separation methodology.

5.2.1: Mathematical Background

For this experiment, a separation approach for flank topographies using CMM measurements as measuring instrument was adapted and used. This approach was proposed in [5], and all mathematical derivations presented in this section are credited to the approach authors.

The three first forms deviations considered in the current work are:

- The 0th order form with the meaning of an offset;
- The 1st order form with the meaning of inclination;
- The 2nd order form with the meaning of curvature.

The third and higher orders deviation can be understood as waviness and will not be considered in this experiment due to the limitations of CT and the uncertainty involved in the process.

The separation and calculation of the concrete parameters of each order can be done by the best-fit approximation and least square method by minimizing the sum of the squares of residuals between deviations δ - as the input data at each separation

step - and the best-fit function s with the parameters x of lower order form deviations. The objective function of least square method is written as follows:

$$f(x) = \sum_{i=1}^n (\delta - s_i)^2 \quad (5.1)$$

5.2.1.1: The 0th order form deviations

The 0th order form deviations have meanings of an offset value or in some cases can be described as a pitch error. Offset deviations can be responsible to several kinds of trouble with the produced part, e.g. a connector that does not fit properly into one product for having a smaller size than the stipulated. The best-fit function for this order can be expressed by one parameter exactly:

$$s_0(x, y) = z_0 \quad (5.2)$$

The deviations used are the current deviations between nominal and actual surfaces.

$$\delta_0 = \delta \quad (5.3)$$

5.2.1.2: The 1st order form deviations

The first order form deviations should be considered as the plane, which has the meaning of inclination of the global topography. Adopting the equation of an arbitrary plane as the best-fit function, the parameters for the 1st order form deviations can be expressed by the parameters of the plane. The general form of an arbitrary plane is written by:

$$Ax + By + Cz + D = 0 \quad (5.4)$$

In this case the domain is considered as the set of pairs (x,y) . Thus we can rewrite the equation of an arbitrary plane as follows:

$$s_1(x, y) = z = ax + by + c \quad (5.5)$$

The deviations values used for the first order are the difference between the nominal deviations and the zero order form.

$$\delta_1 = \delta - s_0(x, y) \quad (5.6)$$

5.2.1.3: The 2nd order form deviations

The parameters for the 2nd order deviations become a set of fundamental forms of the 2nd order and the parameters of scaling transformation, orthogonal transformation (rotation) and parallel translation. Therefore, the second order form deviations can be interpreted as the curvature and anisotropy of the global topography. The general form of a second order surface is given by:

$$a_{11}x_1^2 + a_{22}x_2^2 + a_{33}x_3^2 + 2a_{12}x_1x_2 + 2a_{23}x_2x_3 + 2a_{31}x_3x_1 + 2b_1x_1 + 2b_2x_2 + 2b_3x_3 + c$$

or

$$\sum_{i,j=1}^3 a_{ij}x_ix_j + 2 \sum_{i=1}^3 b_ix_i + c = 0 \quad (a_{ij} = a_{ji}) \quad (5.7)$$

The second order surface can also be expressed in the matrix notation by:

$$s(x) = \tilde{x}^T \tilde{A} \tilde{x} = (\tilde{A} \tilde{x}, \tilde{x}) = 0 \quad (5.8)$$

Where the matrix \tilde{A} and \tilde{x} are given by:

$$\tilde{A} = \begin{pmatrix} A & b \\ b^T & c \end{pmatrix} = \begin{pmatrix} a_{11} & a_{12} & a_{13} & b_1 \\ a_{21} & a_{22} & a_{23} & b_2 \\ a_{31} & a_{32} & a_{33} & b_3 \\ b_1 & b_2 & b_3 & c \end{pmatrix}, \quad \tilde{x} = \begin{pmatrix} x \\ 1 \end{pmatrix} = \begin{pmatrix} x_1 \\ x_2 \\ x_3 \\ 1 \end{pmatrix} \quad (5.9)$$

The second order surfaces can be understood as the points that satisfy the equation when $rank(A)=0$. Moreover, since the second order surface expressed as matrix notation is a quadratic form and A is a real symmetric matrix, it is possible to classify the surfaces in five forms as shown in figure 5.10 [5]:

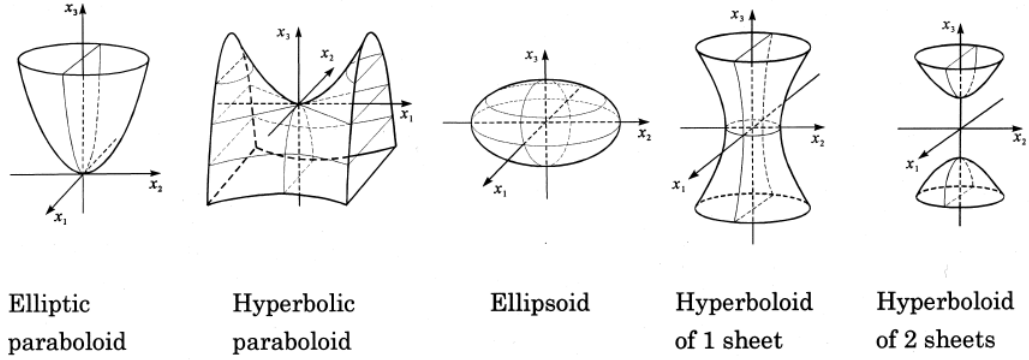


Figure 5.10: Second order surfaces forms.

These geometric forms are described by the following equations:

Name	Equation
Ellipsoid	$X^2 + Y^2 + Z^2 = 1$
Hyperboloid of 1 sheet	$X^2 + Y^2 - Z^2 = 1$
Hyperboloid of 2 sheets	$-X^2 - Y^2 + Z^2 = 1$
Elliptic paraboloid	$X^2 + Y^2 = Z$
Hyperbolic paraboloid	$X^2 - Y^2 = Z$

Table 5.1: Equations for each second order surface form.

This means that an arbitrary surface can be obtained from the proper forms by applying a suitable rotation R , parallel translation Q and scaling transformation S matrices. Where the matrices R , Q and S are given by:

$$S = \begin{pmatrix} S_x & 0 & 0 & 0 \\ 0 & S_y & 0 & 0 \\ 0 & 0 & S_z & 0 \\ 0 & 0 & 0 & 1 \end{pmatrix} \quad Q = \begin{pmatrix} 1 & 0 & 0 & Q_x \\ 0 & 1 & 0 & Q_y \\ 0 & 0 & 1 & Q_z \\ 0 & 0 & 0 & 1 \end{pmatrix} \quad R = \begin{pmatrix} \cos \theta & -\sin \theta \\ \sin \theta & \cos \theta \end{pmatrix} \quad (5.10)$$

Although there are five fundamental forms we can reduce them into two types: a paraboloid and an ellipsoid/hyperboloid function.

The paraboloid equation is given by:

$$z = x^2 \pm y^2 \quad (5.11)$$

After applying the rotation, parallel translation and scaling transformation the equation can be written by:

$$s_2(x, y) = z = \frac{S_z}{S_x^2} [\cos \theta_z x + \sin \theta_z y - Q_x]^2 \pm \frac{S_z}{S_y^2} [-\sin \theta_z x + \cos \theta_z y - Q_y]^2 + Q_z \quad (5.12)$$

In this project the paraboloid function has been chosen as best-fit function for the second order. The paraboloid is enough to evaluate the curvature and the anisotropy of the second order. In addition, it has more stability and is more time saving, as long as it needs to calculate 4 parameters (instead of 7 as in the case ellipsoid/hyperboloid function) [5].

In contrast with the first and zero order, the second order form cannot be solved analytically. For a good approximation the quasi-Newton method can be used with initial values chosen so that:

$$Q_x = Xlength/2, \quad Q_y = Ylength/2, \quad Q_z = 0.0$$

The deviations used for the best fit, in this case, are the difference between the nominal deviations and the sum of the zero order and first order form.

$$\delta_2 = \delta - s_0(x, y) - s_1(x, y) \quad (5.13)$$

5.2.2: SmartInspeCT

With the aid of the software SmartInspeCT, it was possible to extract the deviations of each surface. The SmartInspeCT was implemented in Matlab by WZL for use in this project and was based on the separation methodology described in the previous section.

The software provides a nominal-actual comparison by introducing respectively a CAD model and a point cloud of the sample measured. The CAD model is a .stl (standard stereolithography ASCII) file which is supported in many CAD softwares. On the other hand, SmartInspeCT provides as outputs the deviations by orders and its parameters.

Once both models are loaded in the software and one surface is selected (figure 5.11), it is possible to start running the separation by pressing the 'Separate deviations'

button. After the software calculates the deviations of the surface, a response window appears with the deviation results in each order (figure 5.12).

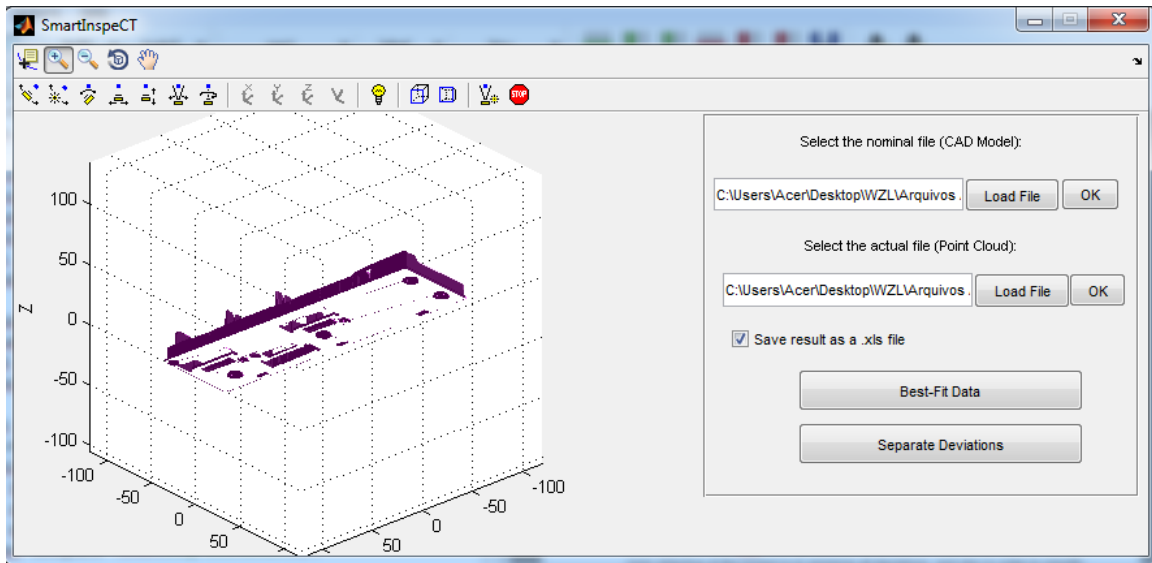


Figure 5.11: SmartInspeCT software with the Bottom surface selected.

The response window shows two results for the offset, four results to the first order, seven results for the second order and two results for third order and superiors, as is shown in table 5.2. In order to simplify the analysis, just the RMS results for offset, first and second orders were considered.

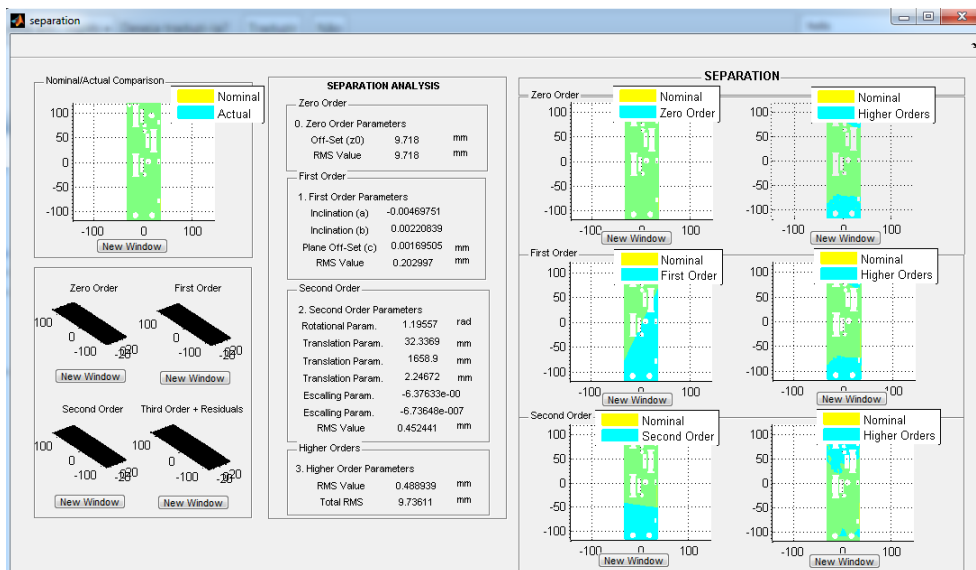


Figure 5.12: SmartInspeCT software results for the Bottom surface selected.

Order	Deviation
0. Order	Off-Set (mm) RMS Value (mm)
1. Order	Inclination(a) Inclination(b) Plane Off-Set (c) (mm) RMS Value (mm)
2. Order	Rotational Param. (Oz) (rad) Translation Param. (Qx) (mm) Translation Param. (Qy) (mm) Translation Param. (Qz) (mm) Escaling Param. (p1) Escaling Param. (p2) RMS Value (mm)
3.+ Order	RMS Value (mm) Total RMS (mm)

Table 5.2: SmartInspeCT software output parameters.

The deviation values were extracted for 6 surfaces (figure 5.13) of the samples and were used in the system's modeling.

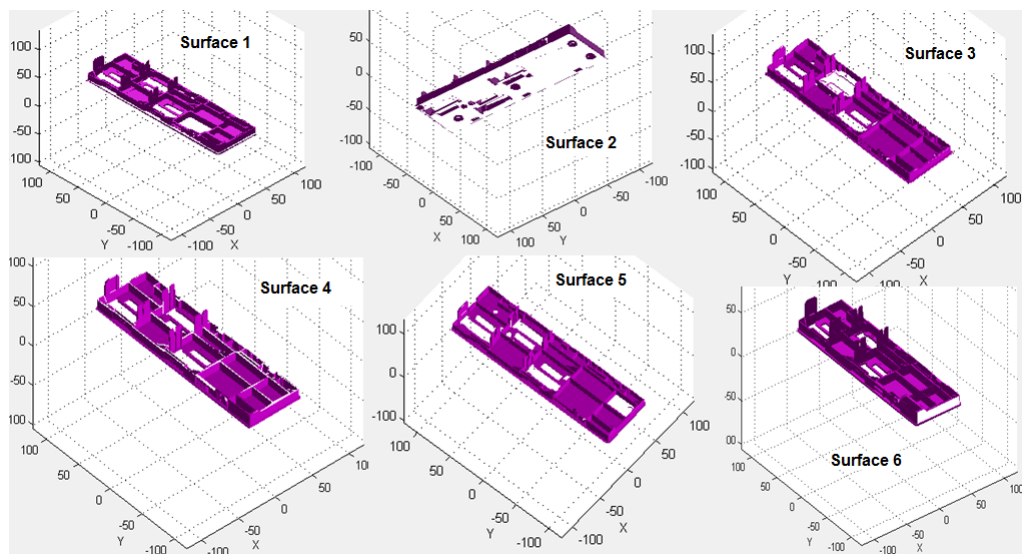


Figure 5.13: Sample surfaces that have been analyzed in the project.

5.3: Modeling

With the aid of the software Matlab, it was possible to perform a full-quadratic regression and propose a response surface modeling. The RMS absolute deviations of the six surfaces were considered to model the system, as well as the four input factors. Their interactions were generated one by one, and all the influences of each factor have been modeled.

For the representation of the model, the abbreviation of table 5.3 was used.

Factors	Abbreviation
Pressure [bar]	P
Pressure time [s]	Pt
Cooling time [s]	Ct
Cooling temp [°C]	CT

Table 5.3: Abbreviations of factors

The response surface model function with all the coefficients and factors influences is presented:

$$\delta = a + b * P + c * Pt + d * Ct + e * CT + f * P * Pt + g * P * Ct + h * P * CT + i * Pt * Ct + j * Pt * CT + k * Ct * CT + l * P^2 + m * Pt^2 + n * Ct^2 + o * CT^2 \quad (5.14)$$

The tables with the coefficients for each order deviations of the six surfaces of interest are presented:

	Surface 1			Surface 2		
Coefficients	Offset	First	Second	Offset	First	Second
a	7.66885	0.34133	0.12016	9.63629	0.01096	1.93990
b	3.13E-4	-4.71E-4	-2.38E-5	0.00121	7.29E-4	-0.00184
c	-0.01032	0.02139	0.42561	0.01643	0,05342	-0,04121
d	0.03777	-0.01291	0.00595	0.04293	0.00908	-0.10346
e	-0.00958	0.00138	-0.01798	-0.01706	-0.00362	-0.01735
f	-1.05E-4	2.39E-5	-1.13E-4	-1.71E-4	1.28E-5	1.03E-4
g	-1.22E-4	6.52E-5	1.34E-4	-1.75E-4	-1.33E-5	-5.23E-6
h	3.32E-5	-1.17E-5	-4.37E-5	3.89E-5	-8.13E-6	2.37E-5
i	-0.00237	9.28E-4	-0.00904	-0.00262	9.09E-4	-8.20E-4
j	3.85E-5	2.46E-5	-4.21E-4	1.05E-4	3.70E-4	-0.00164
k	2.10E-4	-4.67E-5	9.61E-4	4.56E-4	2.83E-4	1.15E-4
l	4.52E-7	2.08E-8	1.78E-6	4.24E-7	-4.62E-7	1.31E-6
m	0.00701	-0.00456	-0.02722	0.00593	-0.00989	0.01298
n	-4.27E-4	-1.23E-4	-0.00139	-6.04E-4	-8.35E-4	0.00343
o	-3.34E-6	1.75E-5	1.32E-4	2.06E-5	-2.94E-6	1.68E-4

	Surface 3			Surface 4		
Coefficients	Offset	First	Second	Offset	First	Second
a	8.16897	0.34972	0.20397	0.56810	0.04105	-0.99065
b	0.00109	-5.23E-5	2.15E-4	-0.00291	-3.38E-4	4.98E-4
c	-0.00836	-0.02064	-0.00693	0.02325	-0.01906	0.13770
d	0.03380	-0.00577	3.93E-4	-0.01230	-5.13E-4	0.07670
e	-0.02225	-0.00275	-0.00114	0.00717	0.00762	0.01775
f	-1.35E-4	-4.56E-6	-1.27E-5	-3.03E-5	-5.72E-5	-9.89E-6
g	-2.18E-4	-9.30E-6	-1.63E-5	-4.20E-5	5.36E-5	2.52E-6
h	5.04E-5	3.6E-6	1.30E-6	2.35E-5	-7.63E-6	5.52E-6
i	-0,00243	4.82E-5	-2.43E-4	-2.44E-4	5.08E-4	6.36E-4
j	2.96E-4	5.18E-5	-2.36E-5	-3.81E-4	-2.48E-4	-0.00111
k	5.26E-4	1.57E-5	-6.70E-6	1.08E-4	-1.86E-4	4.25E-4
l	1.20E-6	2.89E-7	2.69E-7	4.78E-6	-7.60E-7	-1.50E-6
m	0.00678	0.00164	0.00125	4.77E-4	0.00141	-0.01022
n	-2.09E-4	2.06E-4	1.39E-4	4.88E-4	-1.36E-4	-0.00336
o	2.85E-5	1.71E-5	1.40E-5	-1.10E-4	-2.89E-5	-1.94E-4

Coefficients	Surface 5			Surface 6		
	Offset	First	Second	Offset	First	Second
a	6.62451	0.46448	0.46216	5.38921	0.48755	0.40792
b	4.15E-4	-1.95E-4	-1.97E-4	-0.00505	-0.00138	-2.65E-4
c	-0.00663	-0.00627	-0.00687	0.22961	0.01673	0.03219
d	0.06271	-0.02456	-0.02471	0.01703	-0.00724	-0.01926
e	-0.00992	-1.05E-4	-1.78E-5	0.01229	0.00196	0.00494
f	-1.47E-4	-5.26E-5	-5.30E-5	-7.80E-5	1.12E-4	6.90E-5
g	-1.63E-4	2.11E-5	2.19E-5	-2.15E-4	7.31E-6	1.70E-5
h	3.11E-5	5.26E-6	5.34E-6	3.10E-5	6.11E-6	-2.16E-6
i	-0.00376	7.04E-4	7.85E-4	-0.00651	1.48E-4	8.38E-4
j	-3.95E-4	-2.27E-4	-2.35E-4	-9.86E-5	-5.71E-4	-4.53E-4
k	4.34E-4	-4.52E-5	-4.24E-5	1.13E-4	8.10E-5	2.30E-5
l	1.23E-6	-1.22E-7	-1.63E-7	1.51E-5	8.46E-7	-6.79E-7
m	0.01238	0.00164	0.00161	-0.00515	-0.00179	-0.00441
n	-9.77E-4	5.67E-4	5.49E-4	0.00144	8.64E-5	4.65E-4
o	-6.72E-6	7.46E-6	6.50E-6	-1.42E-4	-2.42E-5	-3.51E-5

Table 5.4: Values of coefficients for each deviation order with response surface full quadratic model of Surfaces 1 to 6.

5.4: CT measurements and RSM comparisons

With the coefficients of each surface model, it is now possible to evaluate and validate the models. For this purpose, the four controllable input factors were given as entrances of the response surface model (equation 5.14) and the results were compared with the measured SmartInspeCT values.

In the figures 5.14, 5.15, 5.16, 5.17, 5.18, 5.19 is possible to verify the behavior of the model for the offset (0th degree) on each surface. The figures for first and second orders deviation for each surface are found in appendix C.

In general, the model gave a good representation of reality when compared to the CT measured values, with average relative errors of about 0.47 to 10.87%. The relative errors for all samples deviations of each surface are found in appendix B.

The averages relative errors for the offset deviations are:

- Surface 1 "Inside" - 0.58%;
- Surface 2 "Bottom" - 0.47%;
- Surface 3 "Triple Cavity" - 0.67%;
- Surface 4 "Upper Strip" - 6.64%;
- Surface 5 "Single Cavity" - 0.74%;
- Surface 6 "Right Side" - 1.28%.

These results indicate the response surface model is a good model to describe this type of input-output relationship, especially for the zero order (offset) deviations.

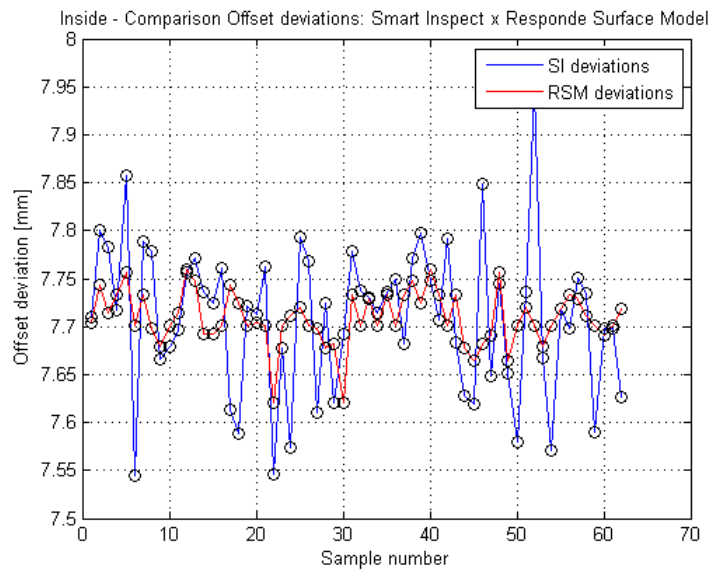


Figure 5.14: Deviation of CT samples measurement and response surface model calculated values for Surface 1.

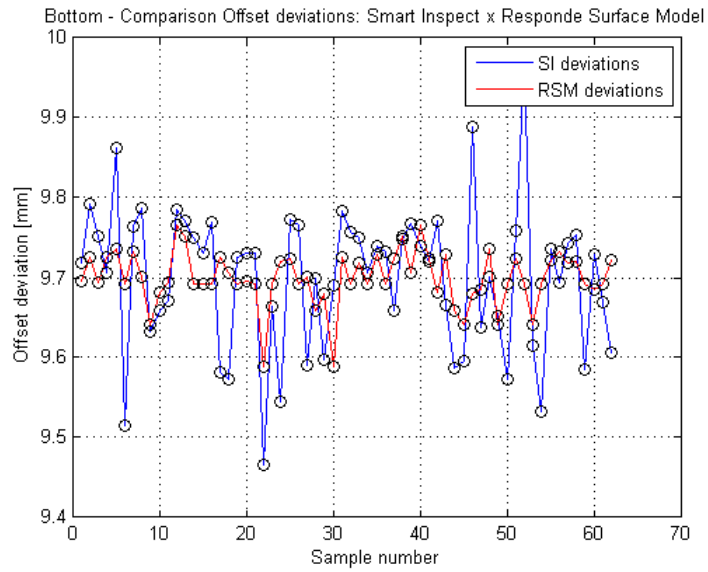


Figure 5.15: Deviation of CT samples measurement and response surface model calculated values for Surface 2.

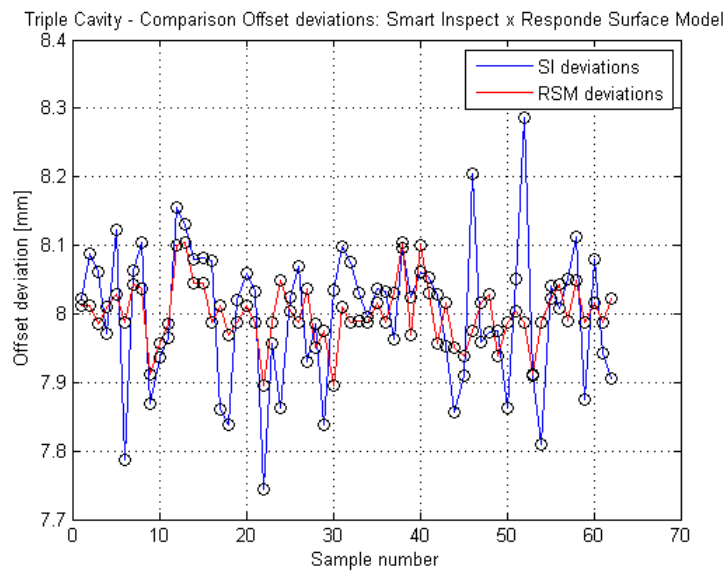


Figure 5.16: Deviation of CT samples measurement and response surface model calculated values for Surface 3.

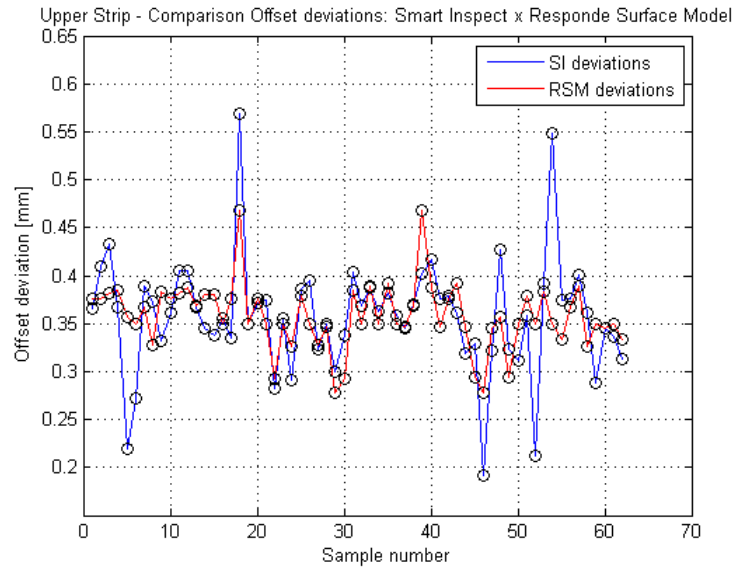


Figure 5.17: Deviation of CT samples measurement and response surface model calculated values for Surface 4.

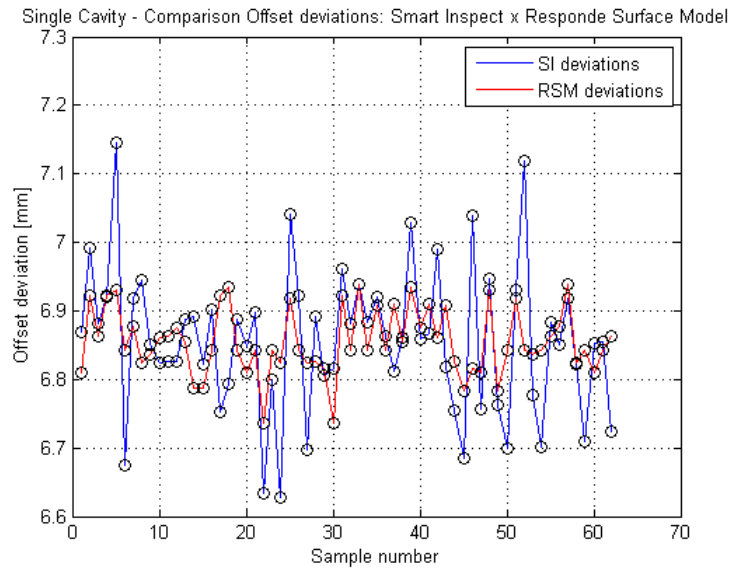


Figure 5.18: Deviation of CT samples measurement and response surface model calculated values for Surface 5.

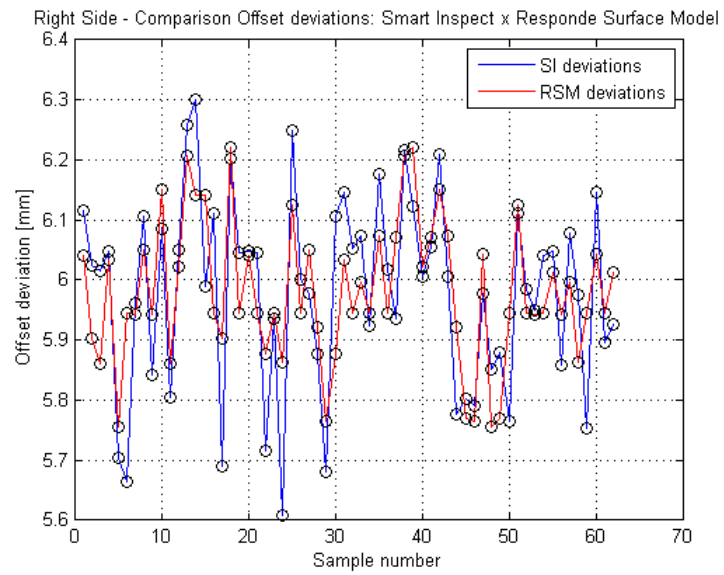


Figure 5.19: Deviation of CT samples measurement and response surface model calculated values for Surface 6.

6 Results and Analysis

After the response surface model was validated for each surface of interest, the model is able to represent the plastic injection system. In this case, it is now possible to perform an analysis of variance in order to verify how the input factors exert influence in each degree of deviation.

Once the model has been evaluated, new inputs were simulated by varying the parameters independently one by one around the central point of the standard reference, from its minimum to maximum. The MATLAB software was used to calculate new outputs and also to generate charts that will assist in the analysis.

In addition, an encoding was adopted due to the parameters variation. This encoding is necessary so that the variation of all factors can be displayed at the same chart. Therefore, the value -1 represents the minimum value, 0 represents the central value and 1 the maximum value of each factor.

Furthermore, an ANOVA with a significance level of 0.05 was also performed with the aid of the software. This significance level means that all factors that have probability lower than this value ($p < 0.05$) are significant. These results are written in blue in the ANOVA result tables.

6.1: Surface 1 - Inside

For the surface "Inside", it can be concluded that the Pressure time exerts some influence in the First and Second orders deviations (figures 6.2 and 6.3), but it can not be considered a critical parameter in the analysis, as well as Pressure, Pressure time and Cooling Time.

ANOVA for Surface 1					
	Degrees of freedom	Sum of squares	Mean squares	F	P
Offset					
Pressure [bar]	4	0.010578	0.002645	0.409092	0.801
Pressure time [s]	4	0.019570	0.004892	0.775761	0.545
Cooling time [s]	4	0.00332	0.000831	0.126052	0.972
Cooling temperature [°C]	4	0.018455	0.004614	0.729309	0.575
First					
Pressure [bar]	4	0.001332	0.000333	0.480276	0.750
Pressure time [s]	4	0.004469	0.001117	1.750209	0.152
Cooling time [s]	4	0.000132	0.000033	0.046038	0.996
Cooling temperature [°C]	4	0.000824	0.000206	0.293391	0.881
Second					
Pressure [bar]	4	0.016673	0.004168	0.261171	0.902
Pressure time [s]	4	0.126153	0.031538	2.246410	0.075
Cooling time [s]	4	0.064656	0.016164	1.069172	0.380
Cooling temperature [°C]	4	0.065202	0.016300	1.078873	0.375

Table 6.1: ANOVA results for Surface 1.

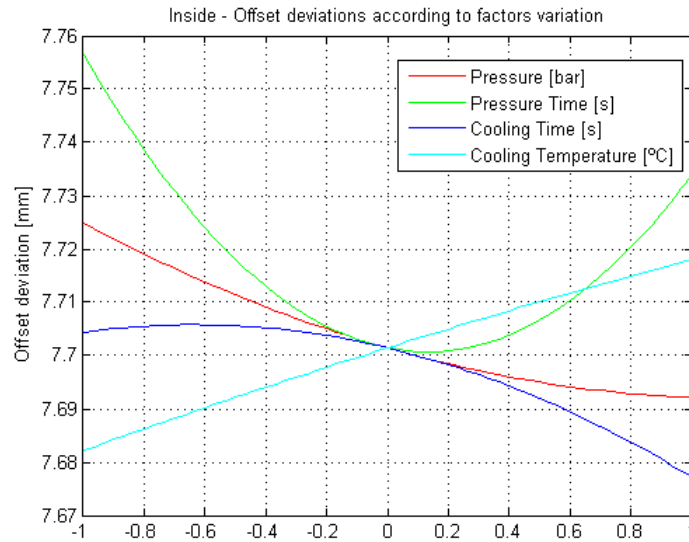


Figure 6.1: Offset order deviations for Surface 1 according to factors variation.

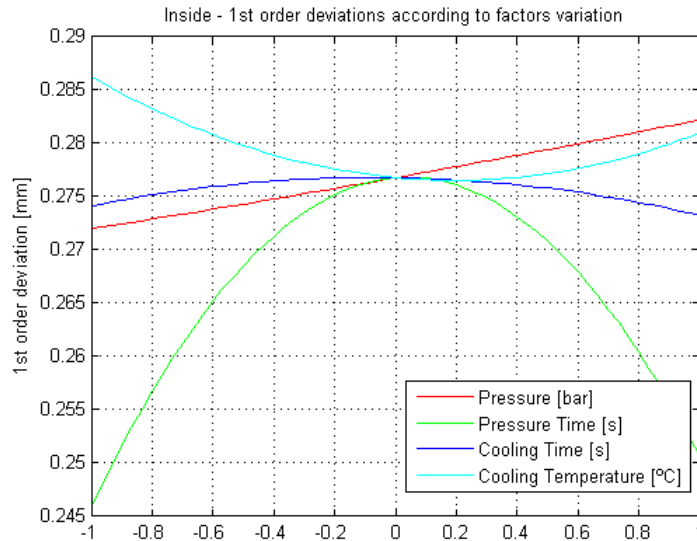


Figure 6.2: First order deviations for Surface 1 according to factors variation.

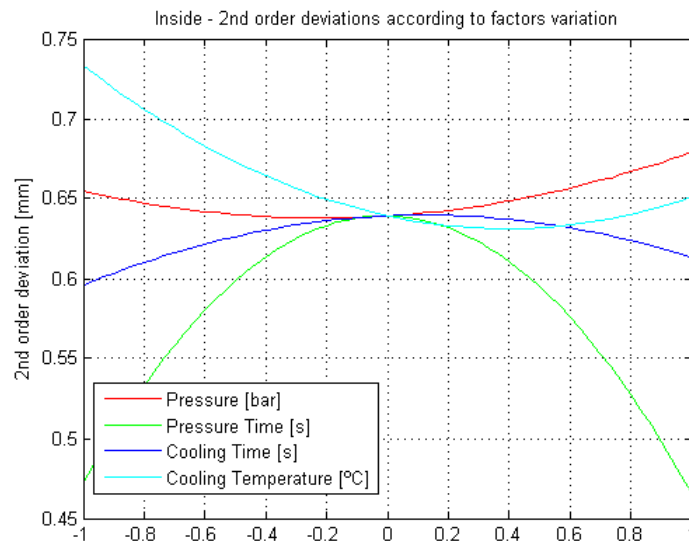


Figure 6.3: Second order deviations for Surface 1 according to factors variation.

6.2: Surface 2 - Bottom

For the 1st order deviations, it can be realized that Pressure time had more influence than the other parameters and is the only significant factor. It can be considered a critical parameter (figure 6.5). On the other hand for the offset and second deviations, the factors are not significant (figures 6.4 and 6.6).

ANOVA for Surface 2					
	Degrees of freedom	Sum of squares	Mean squares	F	P
Offset					
Pressure [bar]	4	0.011309	0.002827	0.323140	0.861
Pressure time [s]	4	0.015729	0.003932	0.453462	0.769
Cooling time [s]	4	0.008356	0.002089	0.237370	0.916
Cooling temperature [°C]	4	0.025618	0.006405	0.753628	0.559
First					
Pressure [bar]	4	0.006735	0.001684	1.793343	0.143
Pressure time [s]	4	0.016690	0.004172	5.459708	0
Cooling time [s]	4	0.008383	0.002096	2.303191	0.069
Cooling temperature [°C]	4	0.007366	0.001841	1.984791	0.109
Second					
Pressure [bar]	4	0.060360	0.015090	1.909567	0.121
Pressure time [s]	4	0.043565	0.010891	1.328712	0.270
Cooling time [s]	4	0.037328	0.009332	1.123466	0.354
Cooling temperature [°C]	4	0.033988	0.008497	1.015774	0.407

Table 6.2: ANOVA results for Surface 2.

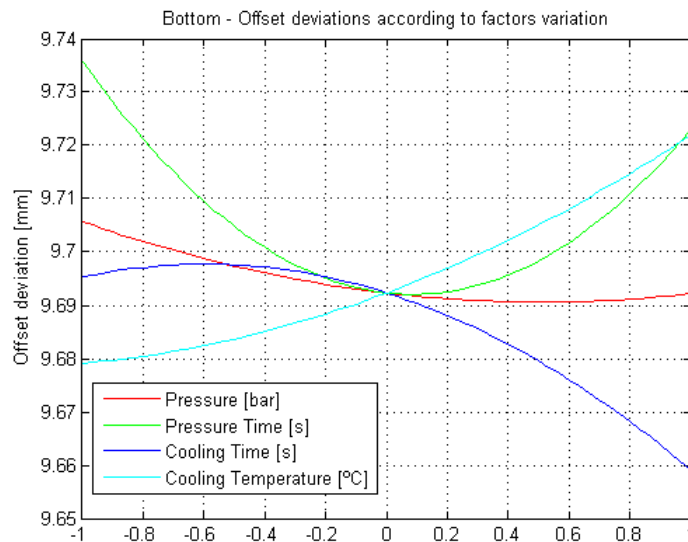


Figure 6.4: Offset order deviations for Surface 2 according to factors variation.

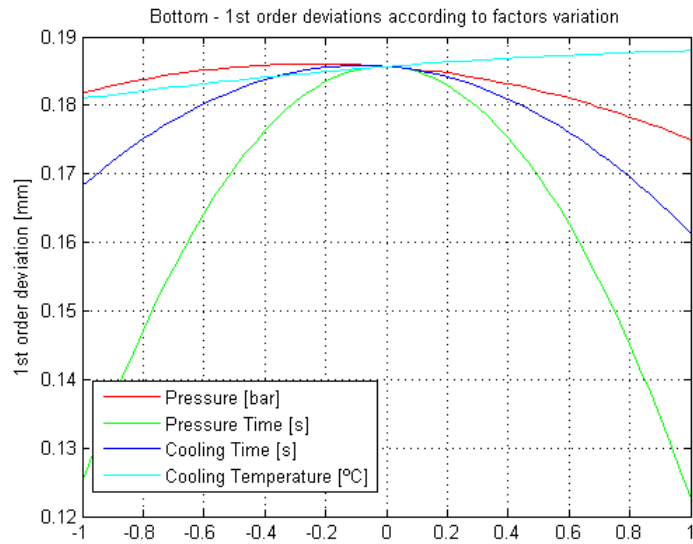


Figure 6.5: First order deviations for Surface 2 according to factors variation.

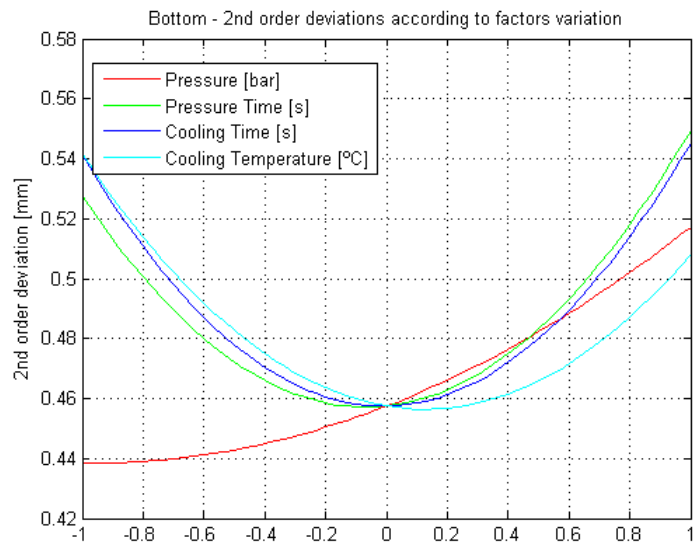


Figure 6.6: Second order deviations for Surface 2 according to factors variation.

6.3: Surface 3 - Triple Cavity

For the offset order deviations, it can be concluded that there aren't significant factors (figure 6.7). Meanwhile for the first order deviations, the four parameters can be considered critical (figure 6.8). For the second order deviations, only Cooling time is not significant (figure 6.9).

ANOVA for Surface 3					
	Degrees of freedom	Sum of squares	Mean squares	F	P
Offset					
Pressure [bar]	4	0.026900	0.006725	0.608670	0.658
Pressure time [s]	4	0.008924	0.002231	0.196317	0.939
Cooling time [s]	4	0.018733	0.004683	0.418449	0.795
Cooling temperature [°C]	4	0.020926	0.005232	0.469053	0.758
First					
Pressure [bar]	4	0.004231	0.001058	8.624108	0
Pressure time [s]	4	0.004638	0.001160	10.039195	0
Cooling time [s]	4	0.002408	0.000602	3.893044	0.007
Cooling temperature [°C]	4	0.002915	0.000729	5.001404	0.001
Second					
Pressure [bar]	4	0.003658	0.000914	6.964683	0
Pressure time [s]	4	0.003433	0.000858	6.346643	0
Cooling time [s]	4	0.001662	0.000416	2.498369	0.053
Cooling temperature [°C]	4	0.002451	0.000613	4.018102	0.006

Table 6.3: ANOVA results for Surface 3.

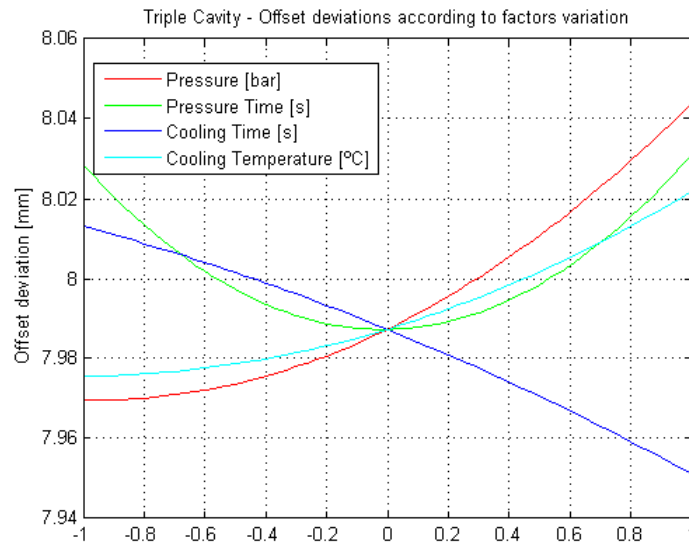


Figure 6.7: Offset order deviations for Surface 3 according to factors variation.

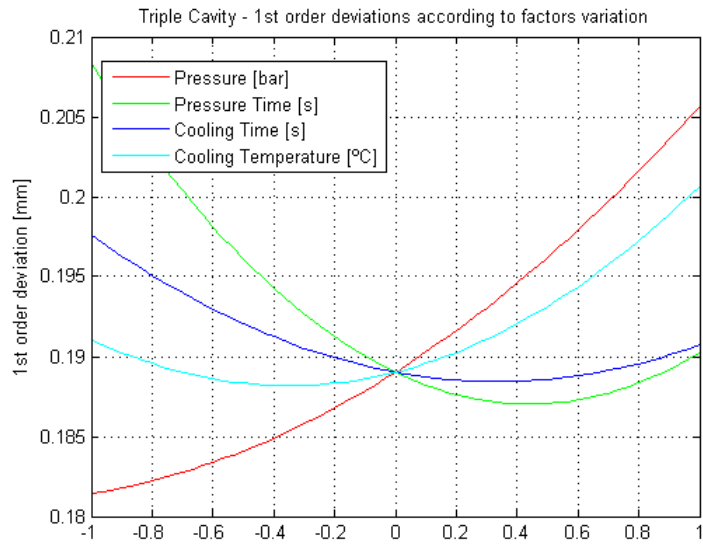


Figure 6.8: First order deviations for Surface 3 according to factors variation.

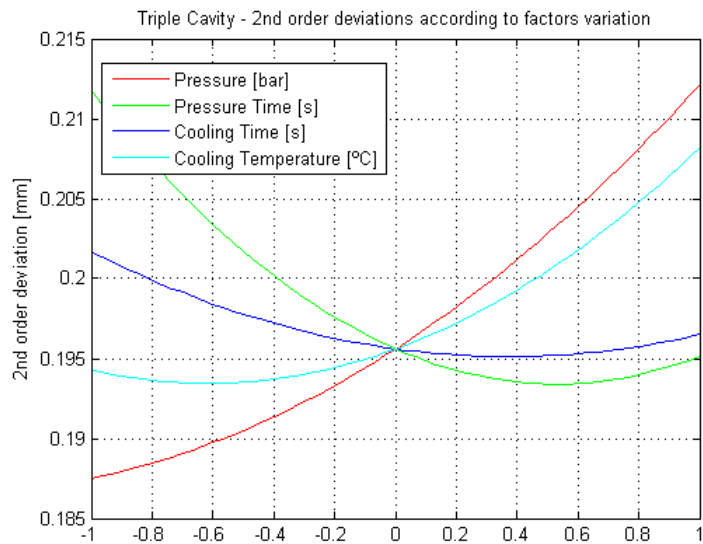


Figure 6.9: Second order deviations for Surface 3 according to factors variation.

6.4: Surface 4 - Upper Strip

For the ffset order deviations, Pressure is the only significant factor (figure 6.10). For the first order deviations, Cooling temperature had more influence than the other parameters and can be considered significant (figure 6.11). For the second order deviations there aren't significant factors.

ANOVA for Surface 4					
	Degrees	Sum of	Mean	F	P
Offset	of freedom	squares	squares		
Pressure [bar]	4	0.050594	0.012648	4.172278	0.005
Pressure time [s]	4	0.007790	0.001948	0.514882	0.725
Cooling time [s]	4	0.006334	0.001584	0.415856	0.796
Cooling temperature [°C]	4	0.029565	0.007391	2.173618	0.083
First					
Pressure [bar]	4	0.001152	0.000288	0.562800	0.690
Pressure time [s]	4	0.002506	0.000626	1.284275	0.287
Cooling time [s]	4	0.002579	0.000645	1.325292	0.272
Cooling temperature [°C]	4	0.004905	0.001226	2.751172	0.037
Second					
Pressure [bar]	4	0.022232	0.005558	1.315590	0.275
Pressure time [s]	4	0.023504	0.005876	1.398241	0.246
Cooling time [s]	4	0.028546	0.007137	1.734688	0.155
Cooling temperature [°C]	4	0.030458	0.007614	1.866071	0.129

Table 6.4: ANOVA results for Surface 4.

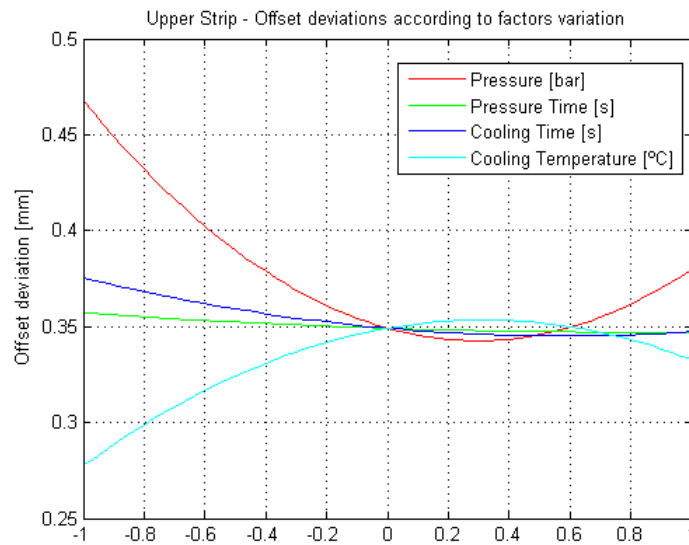


Figure 6.10: Offset order deviations for Surface 4 according to factors variation.

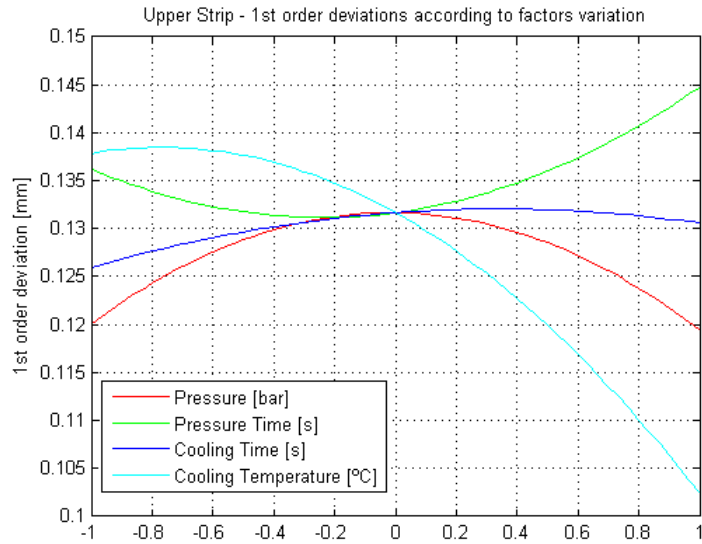


Figure 6.11: First order deviations for Surface 4 according to factors variation.

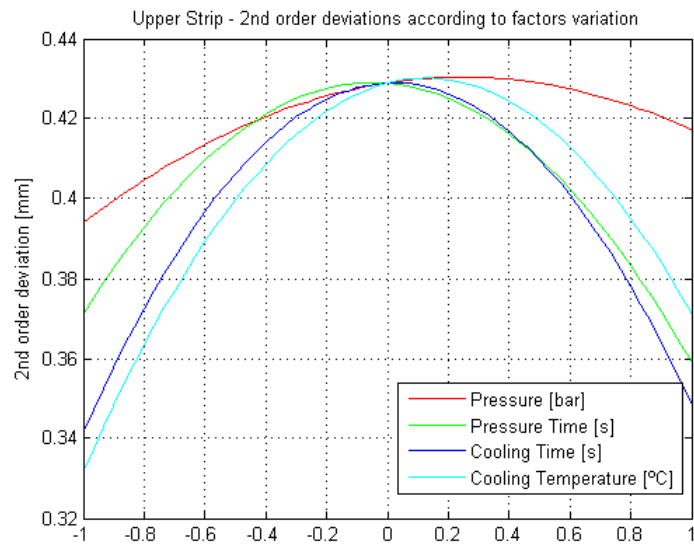


Figure 6.12: Second order deviations for Surface 4 according to factors variation.

6.5: Surface 5 - Single Cavity

For the Surface 5, the parameters Pressure, Pressure time and Cooling time are significant to the first and second orders deviations (figure 6.14 and 6.15). For the first order deviations, there aren't critical factors (figure 6.13).

ANOVA for Surface 5					
	Degrees of freedom	Sum of squares	Mean squares	F	P
Offset					
Pressure [bar]	4	0.083205	0.020801	1.917889	0.120
Pressure time [s]	4	0.085681	0.021420	1.982889	0.109
Cooling time [s]	4	0.010512	0.002628	0.216819	0.928
Cooling temperature [°C]	4	0.050319	0.012580	1.101287	0.365
First					
Pressure [bar]	4	0.004184	0.001046	4.027529	0.006
Pressure time [s]	4	0.004370	0.001093	4.260201	0.004
Cooling time [s]	4	0.003495	0.000874	3.214605	0.019
Cooling temperature [°C]	4	0.002403	0.000601	2.064233	0.097
Second					
Pressure [bar]	4	0.004077	0.001019	3.768077	0.009
Pressure time [s]	4	0.004602	0.001150	4.402648	0.004
Cooling time [s]	4	0.003520	0.000880	3.139829	0.021
Cooling temperature [°C]	4	0.002474	0.000619	2.071571	0.096

Table 6.5: ANOVA results for Surface 5.

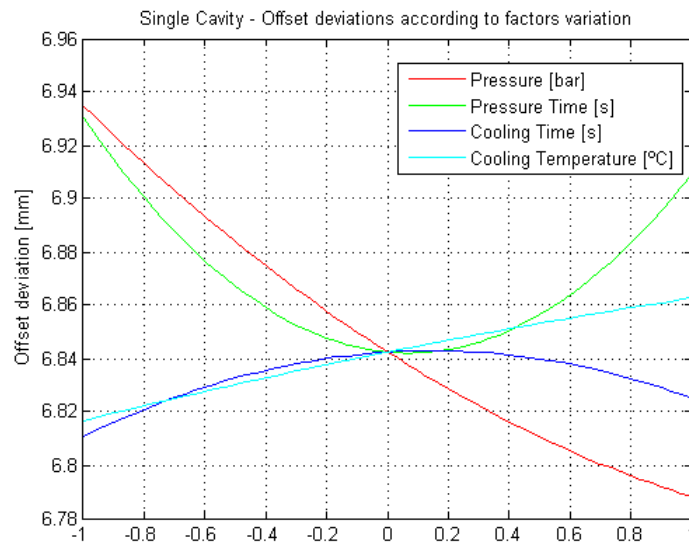


Figure 6.13: Offset order deviations for Surface 5 according to factors variation.

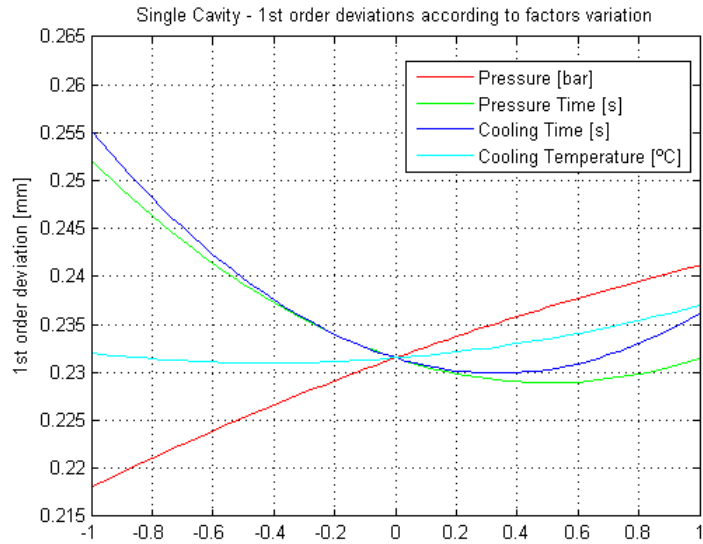


Figure 6.14: First order deviations for Surface 5 according to factors variation.

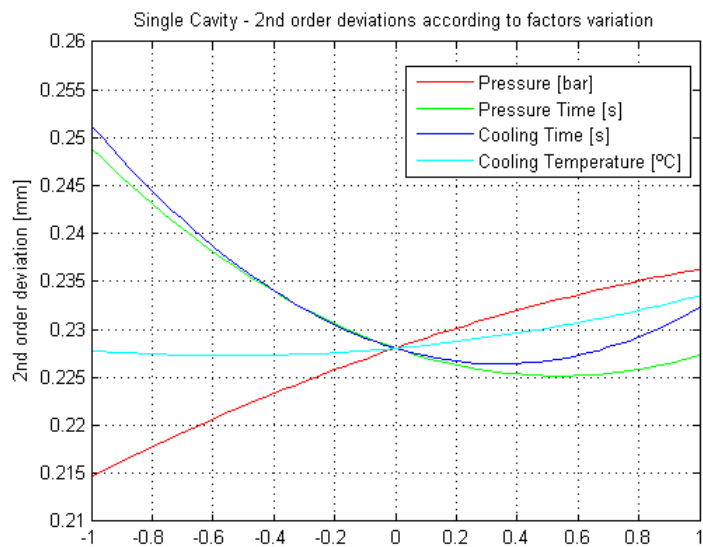


Figure 6.15: Second order deviations for Surface 5 according to factors variation.

6.6: Surface 6 - Right Side

For the offset deviations, the factors Pressure, Pressure time and Cooling temperature are significant (figure 6.16). For the first and second orders deviations there aren't critical parameters (figure 6.14 6.15).

ANOVA for Surface 6					
	Degrees	Sum of	Mean	F	P
Offset	of freedom	squares	squares		
Pressure [bar]	4	0.243497	0.060874	2.613997	0.044
Pressure time [s]	4	0.373487	0.093372	4.444725	0.003
Cooling time [s]	4	0.107639	0.026910	1.048239	0.390
Cooling temperature [°C]	4	0.265739	0.066435	2.901379	0.029
First					
Pressure [bar]	4	0.002458	0.000614	0.439516	0.779
Pressure time [s]	4	0.002148	0.000537	0.382542	0.820
Cooling time [s]	4	0.001177	0.000294	0.207068	0.933
Cooling temperature [°C]	4	0.002224	0.000556	0.396562	0.810
Second					
Pressure [bar]	4	0.002539	0.000635	0.346207	0.846
Pressure time [s]	4	0.005438	0.001360	0.762831	0.554
Cooling time [s]	4	0.004875	0.001219	0.679993	0.609
Cooling temperature [°C]	4	0.004325	0.001081	0.600160	0.664

Table 6.6: ANOVA results for Surface 6.

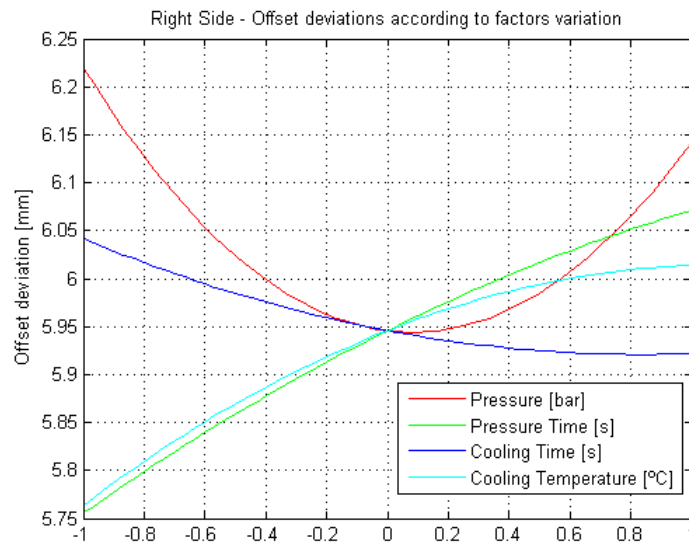


Figure 6.16: Offset order deviations for Surface 6 according to factors variation.

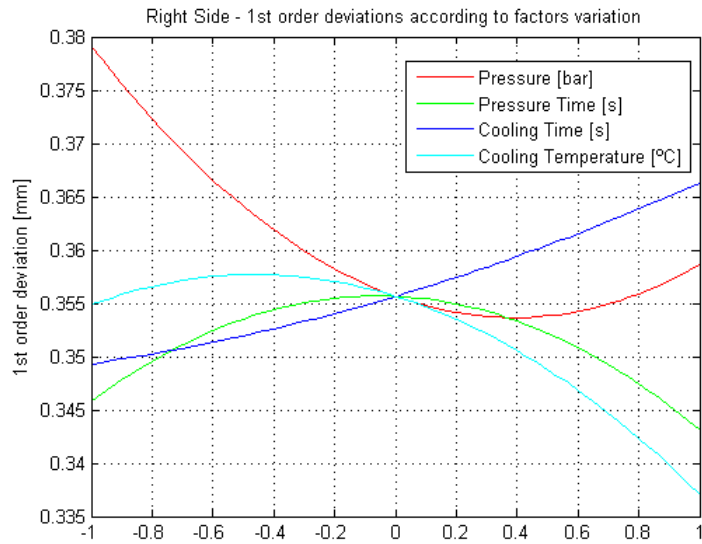


Figure 6.17: First order deviations for Surface 6 according to factors variation.

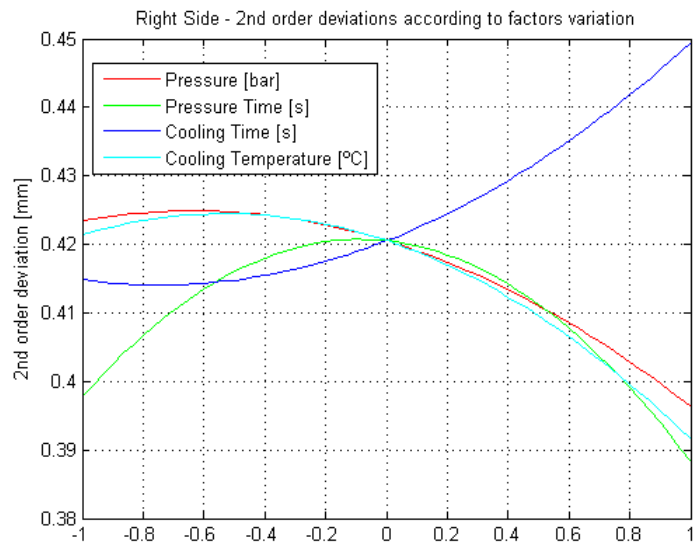


Figure 6.18: Second order deviations for Surface 6 according to factors variation.

6.7: Analysis of production factors

By the presented results, it is possible to conclude that the factors are significant to deviation orders of each surface as follows:

6.7.1: Pressure

- Offset - Surfaces 4 and 6;
- First order - Surfaces 3 and 5;
- Second order - Surfaces 3 and 5.

According to the presented ANOVA results, the factor Pressure is not significant to any deviations order of surfaces 1 and 2. This factor can be understood as a “noise” in the analysis of these surfaces because of its small influence in the final deviation results.

6.7.2: Pressure time

- Offset - Surface 6;
- First order - Surfaces 2, 3 and 5;
- Second order - Surfaces 3 and 5.

The parameter Pressure time is not significant to any deviation order in surfaces 1 and 4. It can be concluded then that this factor represents a noncritical parameter of production and may no longer be considered in the next iteration loops for the analysis of these surfaces.

6.7.3: Cooling time

- Offset - Not significant to any Surface;
- First order - Surfaces 3 and 5;
- Second order - Surface 5.

The parameter Cooling time is not significant in most of the surfaces analyzed. In addition, the factor had a small influence in the offset deviations. As a result this parameter may no longer be considered in the next iteration loops for the analysis of surfaces 1, 2, 4 and 6.

6.7.4: Cooling temperature

- Offset - Surface 6;
- First order - Surface 3 and 4;
- Second order - Surface 3.

The factor Cooling temperature is not significant in Surfaces 1, 2 and 5, i.e., this parameter can be understood as a “noise” in the analysis of these surfaces and may no longer be considered in the next iteration loops for the analysis of these three surfaces.

In the analysis above is also possible to realize that the four factors are not significant to any deviations order of surface 1. Therefore, for a future analysis of this part surface, new controllable factors may be considered in the next DOE.

7 Conclusion

The use of computed tomography proved to be a valuable alternative when measuring inaccessible parts in plastic parts produced by injection molding machines. With the three-dimensional reconstruction and CAD-to-part comparisons, it was possible to extract the deviations by orders and define a new methodology to analyze the deviations on each surface of interest.

It was developed a mathematical model by using the response surface model that was able to “predict” the deviations of the part produced in different orders for each surface. With the analysis of variance (ANOVA), significant variables were isolated for each surface. It was realized that some factors are not significant to any order of deviation and may no longer enter the analysis of the next iteration loop of the process, making it much simpler.

Finally, in the case of Surface 1 “Inside” a DOE with new controllable parameters may be performed in order to analysis which factors exert some influence in its deviations.

8 Future Work

With the aid of the results and analysis presented in this experiment, it is now possible to conduct further design of experiments holding significant parameters in order to increasingly reduce dimensional errors of the surfaces of interest. In the case of Surface 1 “Inside”, a DOE with new controllable factors may be performed in order to analysis wich factors exerts some influence in its deviations. It is noteworthy that even in the case of another type of geometry, it is possible to follow the same methodology adopted to inspect plastic parts produced by injection molding machines.

References

- [1] Robert A. Malloy, "Plastic Part Design for Injection Molding: An Introduction", Munich; Vienna; New York; Hansen, 1994.
- [2] Albert Weckenmann and Philipp Krämer, "Computed tomography for application in manufacturing metrology".
- [3] SmartinspeCT RWTH-Aachen project website , 'http://www.wzl.rwth-aachen.de/cms/www_content/en/5c33489fb6a7c4e2c12579ac005c8273.htm', Accessed in june, 2013.
- [4] Robert Schmitt and Christian Niggemann, "Uncertainty in measurement for x-ray-computed tomography using calibrated work pieces", march, 2010.
- [5] T. Pfeifer, S. Kurokawa, and S. Meyer, "Derivation of parameter of global form deviations for 3-dimensional surfaces in actual manufacturing processes", Vol.29, pp. 179-200, 2001.
- [6] Eriksson, E. Johansson, N. Kettaneh-Wold, C. Wikström, and S. Wold, Umetrics Academy, "Design of experiments - Principles and applications, Third revised and enlarged edition", Umetrics Academy, 2008.
- [7] N. Gelfand, L. Ikemoto, S. Rusinkiewicz and M. Levoy, "Geometrically stable sampling for the ICP algorithm", Proc. 4th International Conference on 3D Imaging and Modeling (3DIM), pp. 260-267, 2003.
- [8] Gary W. Oehlert, "A First Course in Design and Analysis of Experiments", University of Minnesota, 2010.
- [9] Carl Zeiss Industrial Metrology, "Metrotom 1500 CT scanner manual", 2011.
- [10] Ketcham, Carlson, "Acquisition, optimization and interpretation of X-ray computed tomographic imagery: Applications to the geosciences. Computers and Geosciences", 2001.
- [11] Pavel Müller, Jochen Hiller, Angela Cantatore, Markus Bartscher, Leonardo De Chiffre, "Investigation on the influence of image quality in X-ray CT Metrology".

[12] SABIC Innovative Plastics website, '<http://www.sabic-ip.com/gep/en/NewsRoom/PressReleaseDetail/april022012sabicsxenoyiq.html>', Accessed in june, 2013.

[13] Elite Machinery Systems LLC. website, '<http://elitemachinerysystems.com/images/plasticinjection>', Accessed in june, 2013.

Appendix A : DOE worksheet

Sample number	Pressure [bar]	Pressure time [s]	Cooling time [s]	Cooling temp. [°C]
1	225	4.5	10	50
2	162.5	3.25	17.5	40
3	162.5	3.25	12.5	40
4	162.5	5.75	17.5	40
5	225	2	15	50
6	225	4.5	15	50
7	287.5	3.25	17.5	60
8	287.5	5.75	12.5	40
9	162.5	3.25	12.5	60
10	162.5	5.75	12.5	60
11	162.5	3.25	12.5	40
12	287.5	3.25	12.5	60
13	287.5	5.75	12.5	60
14	350	4.5	15	50
15	350	4.5	15	50
16	225	4.5	15	50
17	162.5	3.25	17.5	40
18	100	4.5	15	50
19	225	4.5	15	50
20	225	4.5	10	50
21	225	4.5	15	50
22	287.5	5.75	17.5	40
23	225	4.5	15	50
24	287.5	3.25	12.5	40
25	162.5	5.75	17.5	60
26	225	4.5	15	50
27	287.5	5.75	12.5	40
28	225	4.5	20	50
29	225	4.5	15	30
30	287.5	5.75	17.5	40
31	162.5	5.75	17.5	40
32	225	4.5	15	50
33	162.5	3.25	17.5	60

Sample number	Pressure [bar]	Pressure time [s]	Cooling time [s]	Cooling temp. [°C]
34	225	4.5	15	50
35	162.5	5.75	12.5	40
36	225	4.5	15	50
37	225	7	15	50
38	287.5	5.75	12.5	60
39	100	4.5	15	50
40	287.5	3.25	12.5	60
41	225	7	15	50
42	162.5	5.75	12.5	60
43	162.5	5.75	12.5	40
44	225	4.5	20	50
45	287.5	3.25	17.5	40
46	225	4.5	15	30
47	287.5	5.75	17.5	60
48	225	2	15	50
49	287.5	3.25	17.5	40
50	225	4.5	15	50
51	162.5	5.75	17.5	60
52	225	4.5	15	50
53	162.5	3.25	12.5	60
54	225	4.5	15	50
55	225	4.5	15	70
56	287.5	3.25	17.5	60
57	162.5	3.25	17.5	60
58	287.5	3.25	12.5	40
59	225	4.5	15	50
60	287.5	5.75	17.5	60
61	225	4.5	15	50
62	225	4.5	15	70

Table A.1: DOE worksheet with parameters for samples production

Appendix B : Response surface model relative error (%) compared to measured values

Samples	Surface 1			Surface 2		
	Offset	First	Second	Offset	First	Second
1	0.07642	1.28112	11.86443	0.23386	17.11273	19.63354
2	0.73031	4.40652	10.22155	0.68997	3.83087	4.06067
3	0.87490	10.06759	3.23884	0.59089	23.44008	9.01289
4	0.21141	6.73243	14.90836	0.19897	1.53934	5.59749
5	1.29040	14.40960	13.53647	1.29038	9.06095	12.08540
6	2.08866	14.67046	3.22515	1.86304	25.40201	19.79703
7	0.71125	2.51374	5.90333	0.32624	15.97440	2.63094
8	1.03472	8.59994	5.66707	0.87709	5.88288	2.25929
9	0.18090	3.31813	10.77570	0.10415	16.87628	17.41419
10	0.26812	1.23454	1.78577	0.22817	7.79907	14.59007
11	0.22990	1.55314	11.28387	0.24410	6.01552	10.23216
12	0.03527	1.85024	31.14979	0.19761	10.26540	11.83961
13	0.30099	1.64504	51.18208	0.21109	2.26240	9.02435
14	0.56941	4.81302	1.49727	0.59492	13.96989	65.50867
15	0.41192	3.94809	4.83667	0.40165	2.52352	14.51788
16	0.76689	7.57688	3.27587	0.78171	7.76156	13.86009
17	1.71361	11.87023	17.36717	1.50172	13.56742	36.38433
18	1.79966	14.42257	4.22815	1.38056	19.54531	6.07171
19	0.25606	0.33071	4.18241	0.34686	1.55336	50.81087
20	0.11411	0.57515	16.32315	0.36302	10.47949	8.51024
21	0.78141	8.02428	0.13907	0.39260	37.73421	15.76861
22	0.98265	10.71982	9.85051	1.30884	19.36496	3.42279
23	0.30255	2.20818	6.88048	0.28739	19.58518	18.81456
24	1.82106	13.69768	14.63274	1.83500	9.07258	48.27350
25	0.93334	14.13813	4.20838	0.50111	43.78902	0.85321
26	0.86023	11.14232	1.88476	0.74569	22.55734	16.03780
27	1.15323	6.38636	6.20824	1.15554	10.84736	3.83387
28	0.61469	5.27677	71.98198	0.41515	11.05223	1.58469

Samples	Surface 1			Surface 2		
	Offset	First	Second	Offset	First	Second
29	0.80999	5.60717	10.51933	0.85508	3.02159	11.31656
30	0.94387	14.06008	8.76543	1.05041	3.70952	4.53435
31	0.58659	14.81535	39.57891	0.58551	1.36847	0.84454
32	0.46364	6.96271	8.14136	0.65797	1.07410	64.97699
33	0.01029	0.55528	4.00360	0.32977	18.60573	3.53509
34	0.16058	0.85666	2.97388	0.14066	0.94621	29.46654
35	0.03780	3.21489	2.61250	0.10624	5.19845	1.65534
36	0.62635	6.41587	9.05385	0.41069	18.04531	18.25016
37	0.67053	7.34730	37.82646	0.65901	9.53281	3.19935
38	0.29896	4.10369	12.21575	0.03114	39.35729	6.82803
39	0.93723	8.92264	13.73258	0.62923	21.54753	8.73708
40	0.15611	0.32105	28.76053	0.25626	23.16113	3.14989
41	0.34049	3.83149	32.12164	0.02349	20.03129	4.75063
42	1.17308	6.31383	3.09864	0.92575	2.37214	63.02938
43	0.65098	2.52865	5.61697	0.65691	0.74429	0.68626
44	0.65276	4.06773	8.20334	0.75035	1.46196	0.08079
45	0.57703	2.46731	3.96865	0.48456	4.19553	16.28217
46	2.11613	10.44127	7.16663	2.12597	5.81230	4.87921
47	0.56653	7.56259	18.60503	0.48226	11.17722	21.06892
48	0.14533	0.40711	57.09984	0.36031	19.06901	7.15604
49	0.16155	1.01127	4.90333	0.10792	8.84756	11.96624
50	1.59710	11.62253	12.54990	1.24017	15.96900	2.66604
51	0.19987	3.11741	14.56695	0.35281	10.13336	3.07837
52	3.07790	27.12187	76.66567	2.74591	31.83170	17.07326
53	0.14950	0.00151	77.91047	0.27667	24.56087	8.20769
54	1.73300	16.82518	9.43139	1.67755	17.56738	0.23093
55	0.00198	7.91297	5.71798	0.14805	0.20194	22.55035
56	0.45691	1.28187	5.45177	0.38613	0.49289	1.05778
57	0.27050	2.90163	3.29113	0.25835	13.51295	7.07223
58	0.29538	3.72525	59.49724	0.33866	7.02416	19.79168
59	1.46866	8.63953	12.26506	1.11096	22.79214	5.49272
60	0.09630	4.05116	42.01306	0.46053	7.99908	51.76236
61	0.04695	4.65818	0.19770	0.23180	14.17638	14.99600
62	1.20797	9.80414	10.21416	1.20988	9.45289	12.74557

Samples	Surface 1			Surface 2		
	Offset	First	Second	Offset	First	Second
Bigger (%)	3.0779	27.12187	77.91047	2.74591	43.78902	65.50867
Smaller (%)	0.00198	0.00151	0.13907	0.02349	0.20194	0.08079
Average (%)	0.58181	5.0449	9.24262	0.4714	10.37244	9.01862

Table B.1: Response surface model relative error compared to measured values for Surfaces 1 and 2

Samples	Surface 3			Surface 4		
	Offset	First	Second	Offset	First	Second
1	0.12319	8.30255	6.07516	2.50425	3.89507	1.19996
2	0.94506	0.37170	1.51069	7.94299	25.33451	0.44910
3	0.93519	7.03659	10.28004	11.84849	2.39143	5.46262
4	0.49629	1.58439	2.21699	4.55726	7.95419	6.75328
5	1.16425	17.44097	14.39172	62.94058	3.63121	19.86957
6	2.57782	0.10527	1.24977	28.39003	6.30622	24.47624
7	0.24835	0.11242	1.03422	5.79843	4.02485	18.96406
8	0.82601	2.77585	3.70229	12.14531	2.11103	10.11029
9	0.54264	7.59674	5.91588	15.62848	17.71758	1.93803
10	0.25291	0.80648	0.44545	4.09925	13.26246	3.86828
11	0.25005	3.46592	8.63613	5.96933	3.55201	6.63517
12	0.66513	9.08706	8.01979	4.55056	21.79516	14.61765
13	0.32132	1.41666	1.70021	0.62882	4.06117	3.16108
14	0.44697	15.73190	14.47425	10.01856	8.37414	17.57575
15	0.46763	0.27317	0.71833	12.23528	15.18397	21.23280
16	1.11399	0.01468	0.53322	1.60981	27.99777	14.78268
17	1.92615	5.34709	6.09296	12.28418	15.53132	0.76831
18	1.68791	3.11622	4.91024	17.79041	13.44658	16.41799
19	0.42315	1.63853	0.97610	0.30929	29.02815	10.76690
20	0.5648	1.89489	0.11866	1.19400	26.92818	5.03103
21	0.554	1.60112	0.56504	6.71881	1.54369	23.31713
22	1.96286	1.30261	2.00981	3.89798	14.24802	10.76761
23	0.38792	0.70437	1.47893	1.64269	5.86295	23.87408
24	2.37134	0.72218	1.75097	12.00741	18.08248	4.17379
25	0.23577	14.61622	15.05826	2.19398	10.32093	10.10151
26	1.0056	2.98556	3.44464	11.74365	17.01639	5.57069
27	1.34353	5.75751	5.11898	1.14518	12.05153	8.94720
28	0.43916	4.33399	4.68735	0.51605	3.96442	5.95697
29	1.75111	16.44806	15.20381	7.64931	6.60736	3.27206
30	1.72206	5.08542	4.90100	13.29439	28.16461	7.04454
31	1.06904	0.86415	0.41737	4.66970	20.78810	7.47346
32	1.09453	2.73559	2.30481	5.35593	11.84516	5.17383
33	0.51367	3.83973	3.44631	0.38330	20.83107	23.14461
34	0.10528	4.76007	4.29345	3.59499	0.59457	7.78543

Samples	Surface 3			Surface 4		
	Offset	First	Second	Offset	First	Second
35	0.26225	2.14525	3.00329	2.74353	2.90303	26.97638
36	0.55959	2.02258	1.45776	2.58395	3.54503	5.06297
37	0.8447	4.01602	3.64828	0.58166	1.78724	8.45602
38	0.10641	0.62275	1.71899	0.25202	1.31292	5.87729
39	0.67525	6.90558	5.84877	16.39517	8.19405	5.49399
40	0.4912	3.08364	1.96921	7.24523	11.42831	21.82778
41	0.2846	2.69752	2.32931	7.62604	7.35353	0.41683
42	0.9017	3.18130	3.65004	0.94352	3.31217	2.41384
43	0.78402	1.71769	2.57116	8.74059	2.59967	10.44473
44	1.20501	4.18177	4.47804	9.06367	22.51476	6.18727
45	0.35427	7.81532	6.69115	10.37015	5.38327	0.00268
46	2.79269	3.56917	1.96775	44.27401	1.00882	1.70348
47	0.72085	1.50523	3.11676	7.35241	4.46551	11.59929
48	0.68252	8.71372	7.30366	16.51241	14.90416	14.89280
49	0.46828	6.67735	6.09177	8.63493	20.79365	1.83031
50	1.5836	2.83496	2.98319	11.98577	17.66296	26.33957
51	0.56502	7.27474	6.83338	5.39537	22.14691	8.06436
52	3.6012	0.47890	0.63444	64.60172	23.33235	4.98215
53	0.01394	6.53197	6.43470	2.00301	15.03222	12.72585
54	2.28107	2.74236	3.19093	36.34514	25.57042	7.24124
55	0.2474	2.20956	1.94982	11.20944	0.68953	1.98037
56	0.45207	0.22083	0.04804	2.48360	1.23431	18.93399
57	0.74533	6.08002	4.40982	2.67623	12.01918	11.69365
58	0.79604	6.85001	7.12677	9.88296	25.64392	3.89402
59	1.41456	3.76327	4.76303	21.37307	12.70722	25.94190
60	0.78662	1.01934	3.38623	0.29632	13.38060	19.39102
61	0.55455	7.24876	7.61896	3.72512	8.62971	22.10891
62	1.46689	1.71812	2.05009	6.56193	9.90508	2.02644
Bigger (%)	3.6012	17.44097	15.20381	64.6017	29.02815	26.97638
Smaller (%)	0.01394	0.01468	0.04804	0.25202	0.59457	0.00268
Average (%)	0.67888	3.0346	3.41543	6.64037	10.87462	7.62945

Table B.2: Response surface model relative error compared to measured values for Surfaces 3 and 4

Samples	Surface 5			Surface 6		
	Offset	First	Second	Offset	First	Second
1	0.84321	6.37078	6.43168	1.21038	7.27751	2.85415
2	0.97506	8.92589	10.02690	2.00881	2.435	0.70415
3	0.27074	9.45462	9.45531	2.57608	15.23368	12.20360
4	0.01576	3.55574	3.80791	0.22535	5.09753	7.99482
5	3.01788	9.66094	9.56556	0.90656	2.77978	2.88008
6	2.50467	14.56623	13.67782	4.95715	11.46069	6.26646
7	0.59204	5.45357	5.67576	0.33011	8.52315	6.57916
8	1.73801	4.55844	4.93716	0.88768	10.98699	14.45914
9	0.2338	5.56388	4.62642	1.74494	14.01117	15.05348
10	0.54355	2.10045	1.89608	1.07396	6.14085	10.73995
11	0.53871	0.98603	1.39711	0.93838	3.07865	1.13428
12	0.7117	6.94763	6.98968	0.46254	17.26011	15.45583
13	0.4693	2.83952	4.11193	0.84540	7.45929	1.52150
14	1.51064	11.97603	12.61967	2.52367	4.39745	5.33340
15	0.50861	1.03618	1.05665	2.54149	11.89068	9.06452
16	0.87202	4.74487	4.98353	2.70418	7.83999	2.75535
17	2.53413	8.61135	10.09789	3.72211	5.17162	1.13797
18	2.08043	1.5127	1.88755	0.29806	2.46911	1.80955
19	0.65732	0.67741	1.65693	1.66297	3.1679	0.33620
20	0.54817	3.32022	3.89664	0.09302	14.85342	3.38127
21	0.79013	2.5648	3.79198	1.65681	3.30541	1.67222
22	1.53665	3.58387	3.88793	2.81682	2.45945	5.35067
23	0.63685	6.88595	7.42338	0.15963	12.01553	11.59885
24	2.96993	6.17125	5.69509	4.52153	6.58978	4.06937
25	1.75329	10.50191	11.86885	2.02013	0.00772	0.38061
26	1.14247	4.73686	4.13624	0.91112	8.67691	9.15543
27	1.913	2.42927	3.05445	1.23970	8.91042	9.01407
28	0.97015	5.40226	4.72380	0.75272	10.92703	19.56194
29	0.17578	13.97756	15.01869	1.46440	0.18276	2.92195
30	1.19087	6.35415	6.78468	3.73043	1.26235	1.56788
31	0.55206	4.75271	5.16312	1.81619	11.68912	14.36401
32	0.57836	6.547	6.17848	1.76955	17.09004	7.47221
33	0.0074	2.05758	2.68060	1.25783	6.92471	7.00345
34	0.5999	4.38304	5.10555	0.35791	20.77544	18.52142

Samples	Surface 5			Surface 6		
	Offset	First	Second	Offset	First	Second
35	0.1716	5.82057	6.65631	1.67453	12.65145	11.50602
36	0.29111	7.11849	6.61226	1.20230	6.86246	4.39989
37	1.43468	5.20033	6.07092	2.30277	11.08705	12.34277
38	0.09291	0.89515	0.13231	0.16159	10.10466	9.82598
39	1.33963	3.50091	3.43368	1.58775	4.77561	1.52404
40	0.23558	1.03977	1.23769	0.27421	2.95703	5.19322
41	0.6172	2.14977	2.88557	0.26771	5.59698	4.76180
42	1.8464	2.02668	1.71343	0.94946	2.52626	11.34966
43	1.32751	5.47117	6.04131	1.11320	14.03949	17.77421
44	1.04629	0.71502	0.01144	2.49785	10.31003	12.76248
45	1.4674	6.80009	6.91513	0.57179	9.12558	5.03230
46	3.14736	1.27074	1.62526	0.47336	8.58359	11.90511
47	0.77737	0.42192	0.84471	1.11002	12.4752	14.25223
48	0.2316	8.38577	9.52737	1.63501	15.4285	17.06392
49	0.3149	1.04238	0.91617	1.87039	5.38405	0.31481
50	2.15098	1.81552	2.05012	3.15213	0.38506	0.92256
51	0.18965	7.96524	8.72380	0.21454	4.0395	6.19754
52	3.88356	5.07616	4.81750	0.66667	8.56358	4.65662
53	0.87813	6.96149	6.60361	0.12338	0.06751	0.59026
54	2.12044	8.17223	7.57120	1.58574	12.0457	14.31892
55	0.29391	1.03648	0.28972	0.54970	14.25296	15.12628
56	0.38769	0.86989	0.41212	1.43575	3.17487	1.86305
57	0.29671	4.47871	4.12125	1.32087	15.27243	14.78418
58	0.05845	10.6299	10.94397	1.88436	14.13106	4.63301
59	1.97657	8.08436	8.18556	3.36321	12.83447	11.55347
60	0.63129	3.49411	4.39274	1.66998	6.99387	7.27489
61	0.18517	1.8502	0.84068	0.83371	4.61191	0.54544
62	2.05422	4.82375	4.36048	1.45729	14.61959	15.97201
Bigger (%)	3.88356	14.56623	15.01869	4.95715	20.77544	19.56194
Smaller (%)	0.0074	0.42192	0.01144	0.09302	0.00772	0.31481
Average (%)	0.74454	4.74879	4.77065	1.28935	8.18157	6.42281

Table B.3: Response surface model relative error compared to measured values for Surfaces 5 and 6

Appendix C : Response surface model and SmartInspectCT comparison

Surface 1 - Inside

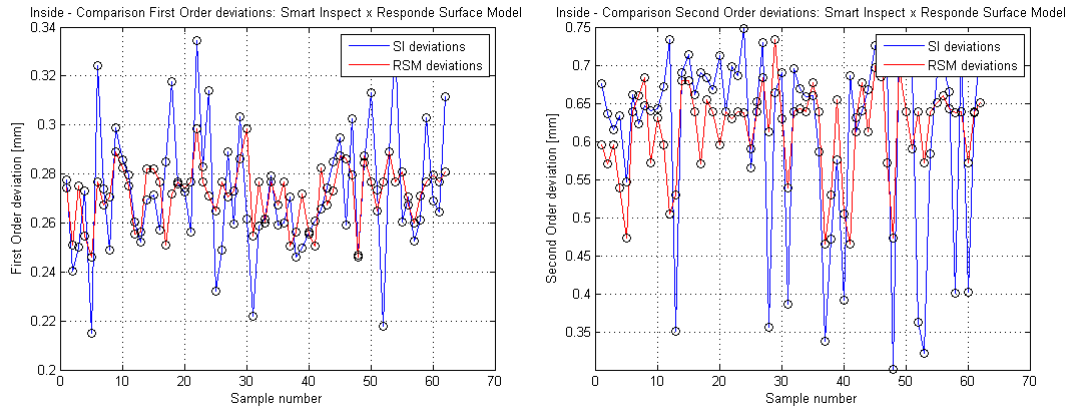


Figure C.1: 1st and 2nd orders deviations of CT samples measurement and response surface model calculated values for Surface 1.

Surface 2 - Bottom

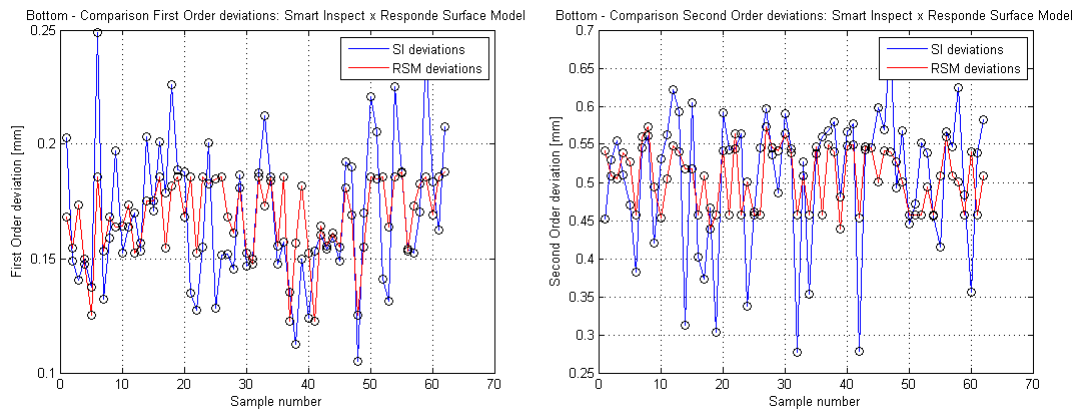


Figure C.2: 1st and 2nd orders deviations of CT samples measurement and response surface model calculated values for Surface 2.

Surface 3 - Triple Cavity

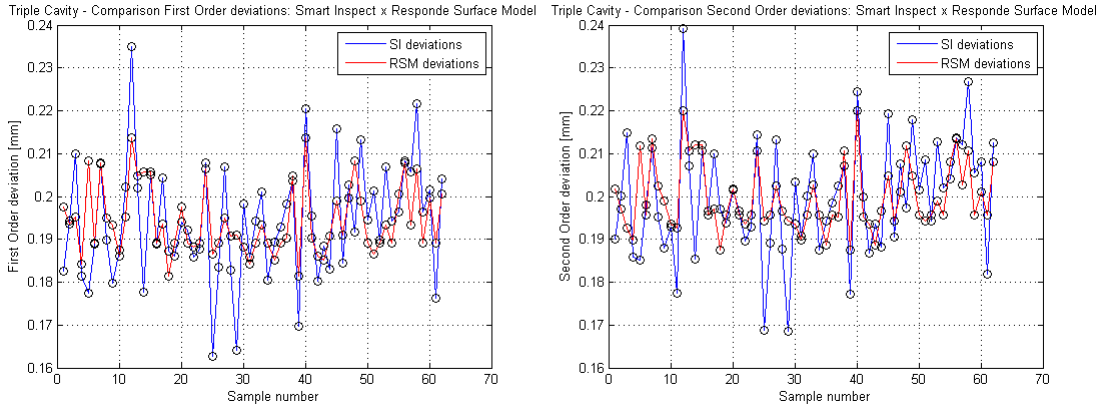


Figure C.3: 1st and 2nd orders deviations of CT samples measurement and response surface model calculated values for Surface 3.

Surface 4 - Upper Strip

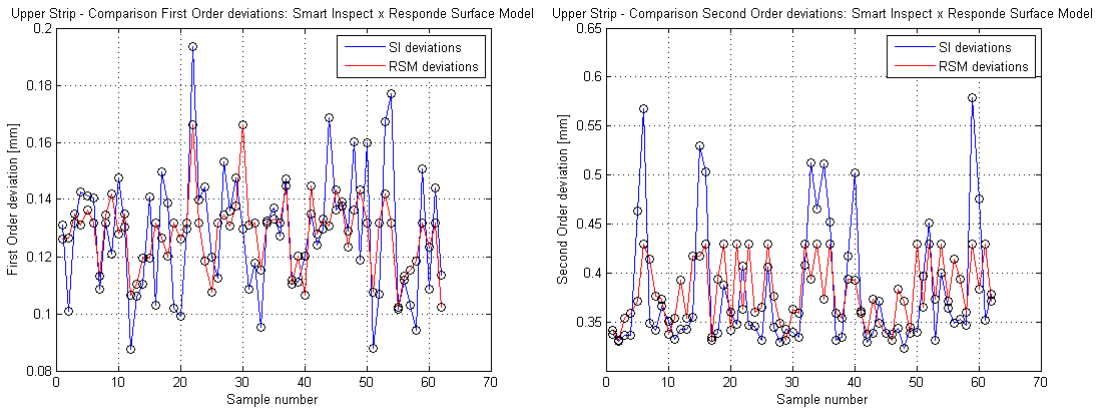


Figure C.4: 1st and 2nd orders deviations of CT samples measurement and response surface model calculated values for Surface 4.

Surface 5 - Single Cavity

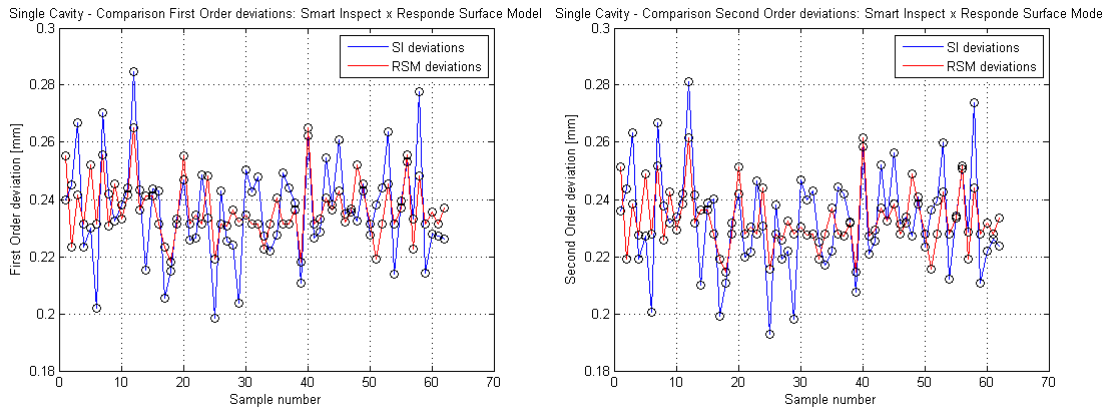


Figure C.5: 1st and 2nd orders deviations of CT samples measurement and response surface model calculated values for Surface 5.

Surface 6 - Right Side

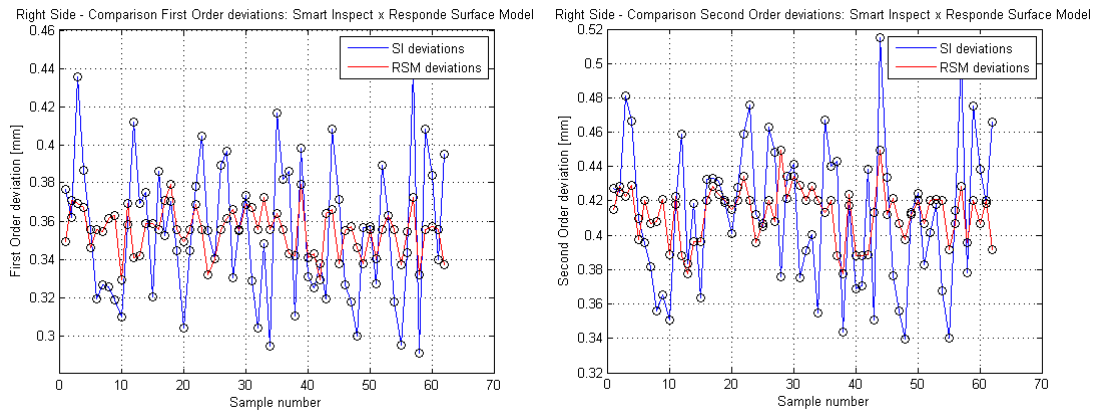


Figure C.6: 1st and 2nd orders deviations of CT samples measurement and response surface model calculated values for Surface 6.